UNIVERZITA PALACKÉHO V OLOMOUCI

Přírodovědecká fakulta

Katedra biotechnologií

Role reaktivních forem kyslíku při tvorbě neutrofilních extracelulárních pastí

BAKALÁŘSKÁ PRÁCE

Autor:	**Marek Buzáš**
Studijní program:	B0512A130007 Biotechnologie a genové inženýrství
Specializace:	Biotechnologie a genové inženýrství
Forma studia:	Prezenční
Vedoucí práce:	**Renuka Ramalingam Manoharan, M.Sc., Ph.D.**
Rok:	2023

PALACKY UNIVERSITY OLOMOUC

Faculty of Science

Department of Biotechnology

Involvement of reactive oxygen species in neutrophil extracellular traps formation

BACHELOR THESIS

Author:	**Marek Buzáš**
Study programme:	B0512A130007 Biotechnology and Gene Engineering
Specialization:	Biotechnology and Gene Engineering
Form of study:	Full
Supervisor:	**Renuka Ramalingam Manoharan, M.Sc., Ph.D.**
Year:	2023

Prohlašuji, že jsem bakalářskou práci vypracoval samostatně s vyznačením všech použitých pramenů a spoluautorství. Souhlasím se zveřejněním bakalářské práce podle zákona č. 111/1998 Sb., o vysokých školách, ve znění pozdějších předpisů. Byl jsem seznámen s tím, že se na moji práci vztahují práva a povinnosti vyplývající ze zákona č. 121/2000 Sb., autorský zákon, ve znění pozdějších předpisů.

V Olomouci dne …….. ……...

Marek Buzáš

I hereby declare that I developed this bachelor thesis on my own with showing all the sources and authorship. I agree with the publication of my thesis by Act. No. 111/1998 Coll., on Higher Education Institutions, as amended. I have been informed that the rights and obligations implied by Act No. 121/2000 Coll., on Copyright and Rights Related to Copyright, as amended, apply to my work.

In Olomouc on …….. ……...

Marek Buzáš

Poděkování

Rád bych vyjádřil upřímné poděkování mé vedoucí Renuce Ramalingam Manoharan, M.Sc., Ph.D. za její trpělivost, pomoc, podporu a zejména za čas, který věnovala naší spolupráci.

Jsem vděčný doc. Ankushi Prasadovi, M.Sc., Ph.D., za jeho velmi cenné rady a za užitečné informace. Rovněž bych chtěl poděkovat doc. RNDr. Michaele Sedlářové, Ph.D z Katedry botaniky za pomoc s konfokální laserovou skenovací mikroskopií. Děkuji také doc. RNDr. Pavlu Pospíšilovi, Ph.D. a všem členům Katedry biofyziky za příjemnou a přátelskou atmosféru v laboratoři.

V neposlední řadě bych chtěl poděkovat své rodině za podporu, pomoc a za to, že tu pro mě všichni vždy byli.

Acknowledgements

I would like to express my sincere gratitude to my supervisor Renuka Ramalingam Manoharan, M.Sc., Ph.D. for her patience, help, support and especially for the time she devoted to our collaboration.

I am thankful to doc. Ankush Prasad, M.Sc., Ph.D. for his very valuable advice and information he gave me. I would also like to thank doc. RNDr. Michaela Sedlářová, Ph.D. from the Department of Botany for her help with confocal laser scanning microscopy. I am also thankful to doc. RNDr. Pavel Pospíšil, Ph.D. and all the members of the Department of Biophysics for creating a pleasant and friendly working environment.

Last but not least, I would like to thank my family for their immense support, help and for always being here for me.

Bibliografická identifikace

Jméno a příjmení autora:	Marek Buzáš
Název práce:	Role reaktivních forem kyslíku při tvorbě neutrofilních extracelulárních pastí
Typ práce:	Bakalářská
Pracoviště:	Katedra biofyziky
Vedoucí práce:	Renuka Ramalingam Manoharan, M.Sc., Ph.D.
Rok obhajoby práce:	2023

Abstrakt

Tato bakalářské práce se zabývá tvorbou reaktivních forem kyslíku (ROS) a jejich vlivem na diferenciaci promyelocytické lidské buněčné linie HL-60 na neutrofily, na aktivaci neutrofilů a na tvorbu neutrofilních extracelulárních pastí (NETs). Neutrofilní extracelulární pasti jsou síťovité struktury tvořené chromatinem a proteiny, které umožňují neutrofilům zachycovat a zneškodňovat patogeny.

Tvorba ROS je jevem spojeným s diferenciací buněčné linie HL-60 na neutrofily a s tvorbou neutrofilních extracelulárních pastí. Nicméně detaily tohoto procesu nejsou zcela objasněné kvůli obtížnosti detekce ROS v živých systémech.

V tomto výzkumu je jako diferenciační činidlo použita kyselina all-trans retinová (ATRA) a jako aktivační činidla jsou využity forbol-12-myristát-13-acetát (PMA) nebo lipopolysacharidy (LPS). Koncentrace těchto činidel, stejně tak jako inkubační doby, se ukázují býti důležitými faktory, které ovlivňují výsledky.

Tvorba superoxidového anion radikálu je detekována pomocí elektronové paramagnetické rezonance s využitím spinové pasti 2-ethoxykarbonyl-2-methyl-3,4-dihydro-2*H*-pyrrol-1-oxidu (EMPO). Ke sledování integrity diferenciovaných buněk je použita konfokální laserová skenovací mikroskopie.

Poslední část našeho výzkumu se zaměřuje na proteinovou analýzu. Proteinové adukty modifikované volnými radikály jsou identifikovány pomocí SDS-PAGE a western blotu s použitím anti-MDA (malondialdehyd) protilátek.

Naše poznatky mohou poskytnout důležité informace pro budoucí výzkum vlivu volných radikálů a jejich aduktů na tvorbu neutrofilních extracelulárních pastí za použití buněčné linie HL-60 jako *in vitro* modelového systému. Zkoumání regulační role

proteinových aduktů při tvorbě neutrofilních extracelulárních pastí by v budoucnu mohlo dopomoci k vývoji nových terapeutických metod.

Klíčová slova:	Neutrofily, neutrofilní extracelulární pasti, reaktivní formy kyslíku, buněčná linie HL-60, buněčná diferenciace, kultivace buněk, kyselina retinová, lipopolysacharidy, forbol-12-myristát-13-acetát, elektronová paramagnetická rezonance, konfokální laserová skenovací mikroskopie, western blot
Počet stran:	58
Počet příloh:	0
Jazyk:	Anglický

Grafický abstrakt

Cíl

Studium tvorby reaktivních forem kyslíku a jejich vlivu na diferenciaci promyelocytické lidské buněčné linie HL-60 na neutrofily, na aktivaci neutrofilů a na tvorbu neutrofilních extracelulárních pastí.

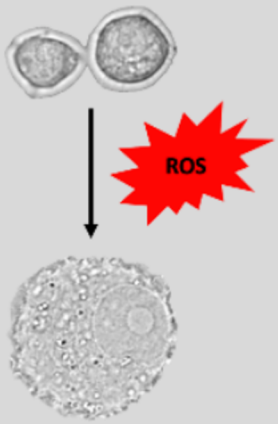

Metody

Po diferenciaci HL-60 buněk na neutrofily (ATRA) a po následné aktivaci neutrofilů (PMA, nebo LPS) byla tvorba ROS sledována různými metodami (EPR se spinovou pastí, konfokální laserová skenovací mikroskopie, western blot).

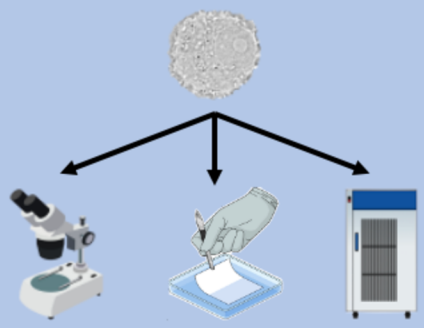

Výsledky

Tvorba superoxidových anion radikálů byla potvrzena EPR detekcí se spinovou pastí. Adukty proteinů modifikované volnými radikály byly detekovány metodou western blot a byly pozorovány rozdíly v intenzitě proteinových pásů.

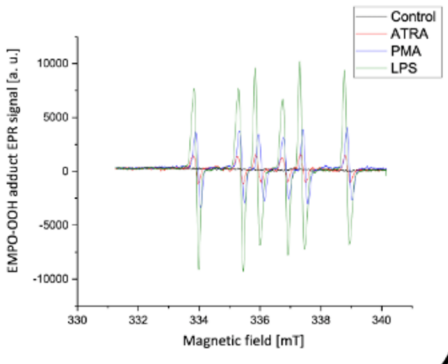

Bibliographical identification

Author's first name and surname:	Marek Buzáš
Title:	Involvement of reactive oxygen species in neutrophil extracellular traps formation
Type of thesis:	Bachelor
Department:	Department of Biophysics
Supervisor:	Renuka Ramalingam Manoharan, M.Sc., Ph.D.
The year of presentation:	2023

Abstract

This bachelor thesis examines reactive oxygen species (ROS) generation and their effect on the differentiation of the promyelocytic human cell line HL-60 into neutrophils, neutrophil activation and neutrophil extracellular traps (NETs) formation. Neutrophil extracellular traps are web-like structures made of chromatin and proteins that allow neutrophils to trap and kill extracellular pathogens.

ROS generation is a phenomenon associated with the differentiation of the HL-60 cell line into neutrophils and neutrophil extracellular traps formation, but the details remain unclear due to the difficulties connected with the detection of ROS in living systems.

For our research, all-trans retinoic acid (ATRA) is used as a differentiating agent and phorbol-12-myristate-13-acetate (PMA) or lipopolysaccharides (LPS) as a stimulus. The concentrations of these agents, as well as the incubation times, appear to be crucial factors that influence the results.

Superoxide anion radical formation is detected by electron paramagnetic resonance spin trapping using 2-ethoxycarbonyl-2-methyl-3,4-dihydro-2*H*-pyrrole-1-oxide (EMPO) as a spin trap. Confocal laser scanning microscopy is utilized to observe the integrity of differentiated cells.

The last part of our research focuses on protein analysis. Free radical modified protein adducts are identified by western blotting using anti-MDA (malondialdehyde) antibodies.

Our findings may provide useful information on the involvement of free radicals and their adducts in NETs formation using HL-60 cell line as an *in vitro* model system. Exploring the regulatory role of protein adducts in NETs formation may support the development of new therapeutic methods in future.

Keywords:	Neutrophils, reactive oxygen species, neutrophil extracellular traps, HL-60 cell line, cell differentiation, cell cultivation, retinoic acid, lipopolysaccharides, phorbol-12-myristate-13-acetate, electron paramagnetic resonance, confocal laser scanning microscopy, western blotting
Number of pages:	58
Number of appendices:	0
Language:	English

Graphical abstract

Aim

Investigate the generation of reactive oxygen species and their effect on the differentiation of the promyelocytic human cell line HL-60 into neutrophils, neutrophil activation and neutrophil extracellular traps formation.

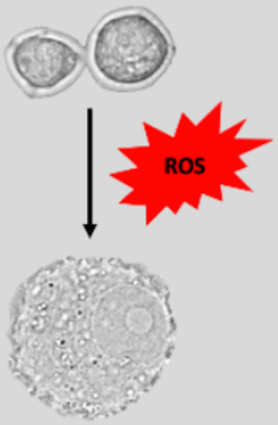

Methods

Post differentiation (ATRA) and neutrophil activation (PMA or LPS), ROS generation was monitored by different methods (EPR spin trapping, confocal laser scanning microscopy, western blotting).

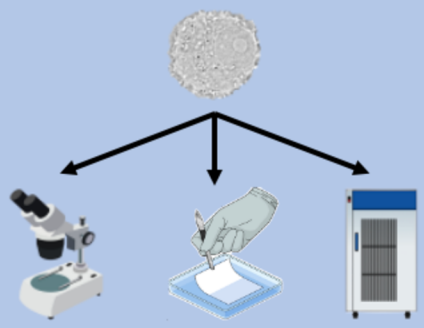

Results

Superoxide anion radical generation was confirmed by EPR spin trapping detection. Free radical modified protein adducts were detected by western blotting and differences in protein band intensity were observed.

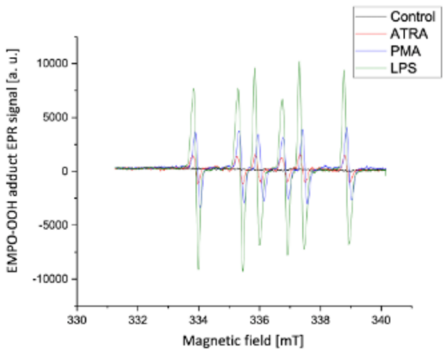

CONTENT

AIMS OF THE THESIS

Theoretical part

1. Writing up an overview of the publications about human myeloid leukaemia cell lines (HL-60, THP-1, U-937), and their differentiation into neutrophils and macrophages, respectively. Generation of reactive oxygen species and its protein adducts characterization with immuno-spin trapping.

Experimental part

1. Learning techniques related to cell culture, its maintenance and cytotoxicity assays using a monocytic cell line model HL-60.
2. Learning protocols related to differentiation of the human myeloid leukaemia cell line HL-60 into neutrophils using chemical (ATRA, PMA) and bacterial (LPS) stimuli.
3. Performing spectroscopic techniques (electron paramagnetic resonance) and confocal laser scanning microscopy.
4. Learning techniques like total protein extraction from cultured cell lines, protein quantification and detection of the free radicals modified protein adducts by western blotting analysis.
5. Evaluation of the measured results and discussion of the results with the literature.

1 INTRODUCTION

Neutrophils are reported to be the most common and abundant leukocytes. They are the primary cells recruited to the site of infection and play a vital role in innate immunity (Rosales *et al.*, 2016). One of the strategies that neutrophils use to neutralize pathogens is neutrophil extracellular traps (NETs) formation. NETs are extracellular web-like structures made of chromatin and proteins (Thiam *et al.*, 2020). DNA in the fibres is mainly from the nucleus but it can also have a mitochondrial origin (Lood *et al.*, 2016).

In this study, the HL-60 cell line was used as an *in vitro* neutrophil model to study the involvement of reactive oxygen species along its differentiation and extracellular traps formation. HL-60 is a promyelocytic cell line derived from a 36-year-old female patient with acute promyelocytic leukaemia (Koyama *et al.*, 2015).

HL-60 cells can be differentiated into neutrophils using chemical stimulants, e.g. all-trans-retinoic acid (ATRA) (Tasseff *et al.*, 2017). These cells can also be differentiated into macrophages using phorbol-12-myristate-13-acetate (PMA) (Mandic *et al.*, 2022). Differentiation into monocytes using dimethyl sulfoxide (DMSO) has also been documented (Zamani *et al.*, 2013). Differentiated neutrophils are induced by a chemical stimulant, e.g. PMA (Manda-Handzlik *et al.,* 2018), or by a bacterial stimulant, e.g. lipopolysaccharides (LPS). Different concentrations of these agents highly affect the differentiation and activation processes. The effect of incubation times should also not be overlooked.

Activated neutrophils produce pro-inflammatory cytokines that are important for immune responses (Tecchio *et al.*, 2014). The most important cytokines include interleukin-1 beta (IL-1β), tumour necrosis factor alpha (TNF-α) or interleukin-8 (IL-8). These pro-inflammatory cytokines are produced at higher levels by neutrophils and monocytes, e.g. during type 2 diabetes (Carestia *et al.*, 2016).

Differentiation of HL-60 into neutrophils leads to reactive oxygen species (ROS) production. Superoxide anion radical is produced by NADPH oxidase (NADPH oxidase, NOX, EC 1.6.3.1) complex, mainly by NADPH oxidase 2 (NOX2). In this scenario, phagocytized organisms are killed by an oxidative burst (El-Benna *et al.*, 2016). Reactive oxygen species are involved in NETs formation (NETosis) (Keshari *et al.*, 2013). The mechanism of ROS-mediated NETosis induction has not been understood, yet. However, it is likely that NETosis is induced due to DNA damage caused by ROS formation during neutrophil activation (Azzouz *et al.*, 2021). ROS generation can be monitored by electron

paramagnetic resonance (EPR) using spin trapping (Nawab *et al.*, 2017) and also by confocal laser scanning microscopy (Ding *et al.*, 2018).

Differentiation into neutrophils is connected with changes in gene expression and protein composition (Rincón *et al.*, 2018). The intracellular events associated with ROS production during NETs formation remain elusive. Malondialdehyde (MDA), a lipid peroxidation product, forms adducts with proteins and these changes can be monitored by various methods (Mas-Bargues *et al.*, 2021). In this work, SDS-PAGE and western blotting were the mainly used techniques. The method involves the identification of malondialdehyde protein adducts formed along the differentiated and stimulated neutrophils.

2 CURRENT STATE OF THE TOPIC

2.1 Neutrophils

2.1.1 Overview of neutrophils

Neutrophils are classified as a type of white blood cells prevalent in the human body and can make up to 70% of all leukocytes. Neutrophils, together with basophils and eosinophils, are members of the group of polymorphonuclear leukocytes (PMNs) (Malech *et al.*, 2014). Their characteristic multilobulated shape of the nucleus (Fig. 1) distinguishes them from other leukocytes. Neutrophils role in the immune system lies in the early response to acute infection by pathogens, mainly bacteria (Hidalgo *et al.*, 2019). However, the antimicrobial activity of neutrophils can lead to tissue damage in the host organism (Soehnlein *et al.*, 2017), such as toxic effects on neurons and the consequent impairment of cognitive functions (Chen *et al.*, 2022).

Neutrophils are formed from the hematopoietic stem cells in the bone marrow, where they are also stored and form the bone marrow reserve. In case of need, e.g. inflammation caused by an infection, neutrophils are quickly mobilised and released into the bloodstream. During this mobilisation, neutrophils must cross a barrier of the sinusoidal endothelium (Hyun & Hong, 2017). The half-life of neutrophils in circulation was usually considered to be around 8 h. Nevertheless, some more recent sources indicate that it can be as long as 5 d or even longer (Lahoz-Beneytez *et al.*, 2016).

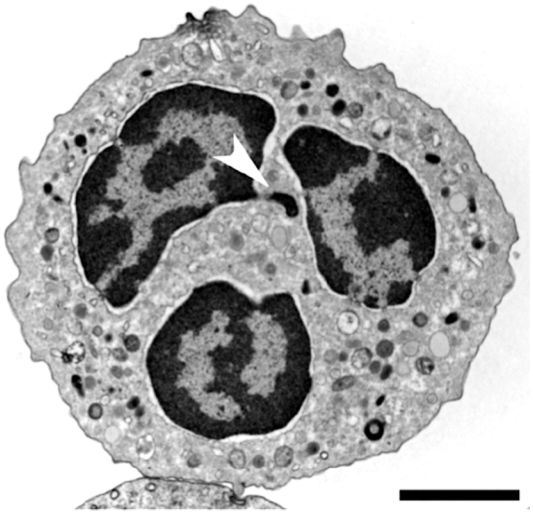

Figure 1. Transmission electron microscopy (TEM) image of a human neutrophil with a multilobulated nucleus. White arrow indicates an inactivated chromosome X (female donor). Scale bar: 2 μm. Adapted from: Brinkmann & Zychlinsky (2012).

2.1.2 Neutrophil granules

In neutrophils, four types of granules (Fig. 2A) can be found: azurophilic (primary), specific (secondary), gelatinase (tertiary), and secretory (quaternary). All of them are formed in the process of differentiation. Azurophilic granules (Fig. 2B) serve as a storage site for toxic mediators, e.g. elastase, myeloperoxidase or cathepsins. Substances stored in the azurophilic granules are important for phagocytosis (DeLeo & Allen, 2020). Specific granules (Fig. 2C) contain antibacterial proteins, such as lactoferrin, cathelicidin or lysozyme. Gelatinase granules are associated with the presence of lysozyme and the proteases gelatinase and leukolysin. Secretory granules abound with a large number of transmembrane receptors, e.g. a TNF receptor. These receptors are incorporated into the plasma membrane during exocytosis. These granules do not harbour many antibacterial proteins (Ramadass & Catz, 2016). However, the cationic antimicrobial protein of 37 kDa (CAP37) may be present (Kasus-Jacobi *et al*., 2020).

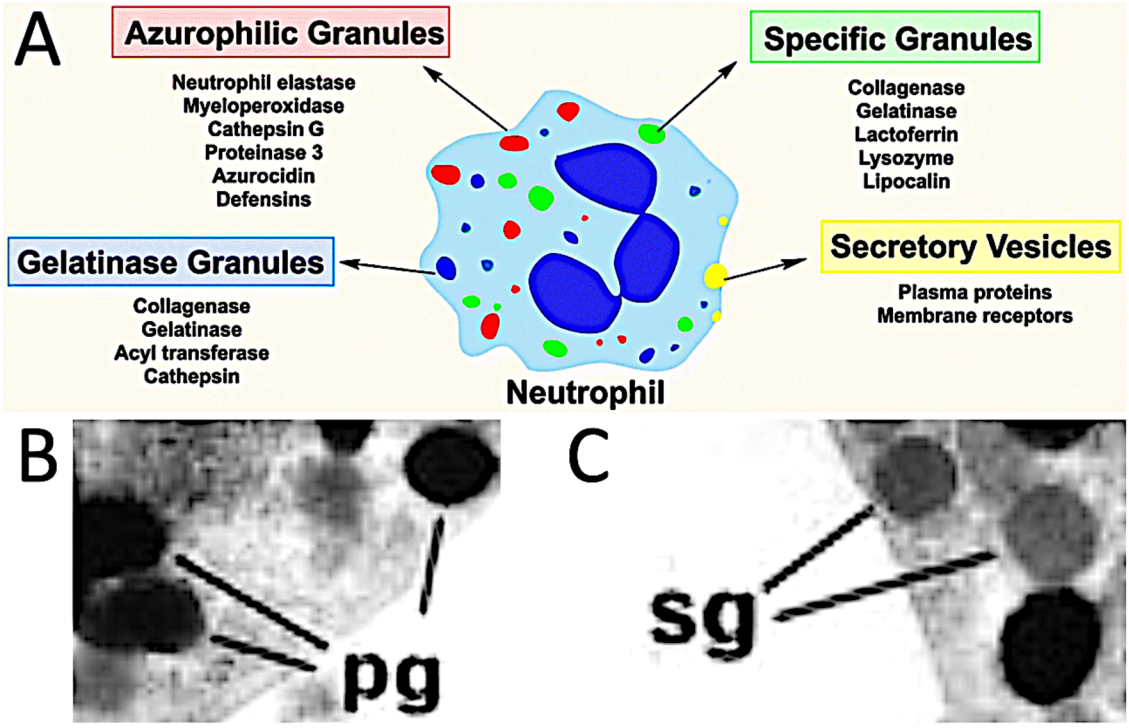

Figure 2. Neutrophil granules. **(A)** Schematic representation of four types of neutrophil granules: primary (azurophilic), secondary (specific), tertiary (gelatinase), and quaternary (secretory). **(B)** TEM image of primary granules **(pg)**. **(C)** TEM image of secondary granules **(sg)**. Modified according to: **(A)** Rawat *et al*. (2021), **(B, C)** Witko-Sarsat *et al*. (2000).

2.1.3 Neutrophils and cytokines

During inflammation, neutrophils are attracted to the site of infection by chemical signals (chemotaxis) produced by the damaged tissue as well as microorganisms (Hasan *et al.*, 2016). Cytokines play an essential signalling role in the neutrophil fight against infection and fulfil two functions (Turner *et al.*, 2014). Firstly, cytokines at the site of infection, e.g. IL-8 or TNF-α, attract neutrophils to the affected area (Duque & Descoteaux, 2014). Secondly, cytokines produced by the neutrophils themselves serve as attractants that draw the attention of other immune cells (Rosales, 2018). Although the cytokines produced by neutrophils can be classified according to several criteria, the division into pro-inflammatory and anti-inflammatory has become the most widely used (Bordon *et al.*, 2013). Pro-inflammatory cytokines include, e.g. IL-1 β, IL-6 or TNF-α. Anti-inflammatory cytokines are, e.g. IL-4, IL-10 or interferon-α (Maspi *et al.*, 2016).

2.1.4 Pathogen neutralization

Neutrophils are considered the first line of defence in the innate immune system, wherein they capture and destroy invading pathogens (bacterial, fungal, and viral) through phagocytosis, intracellular degranulation or formation of NETs (Gazendam *et al.*, 2016; Storisteanu *et al.*, 2017; Ma *et al.*, 2021).

Phagocytosis is a process involved in the elimination of pathogens or particles that can cause disease (Schumann, 2016). Prior to the beginning of phagocytosis, targeted particles are opsonized – extracellular proteins opsonins are attached to the surface of the particles (Garcia-Senosiain *et al.*, 2021). The targeted particle is internalized (Fig. 3) and a phagosome is subsequently formed. The internalization process is achieved either through plasma membrane protrusions that non-specifically surround adjacent particles or via sequential binding of surface receptors to the particle's ligands, leading to the wrapping of the whole particle by the plasma membrane through the zipper mechanism (Jaumouillé & Waterman, 2020).

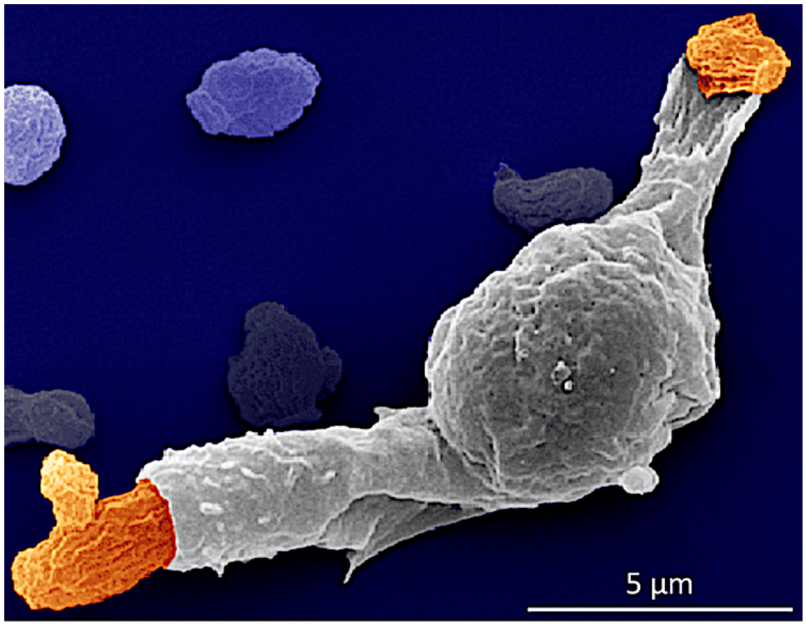

Figure 3. Pseudocolor scanning electron microscopy (SEM) image of a human neutrophil internalizing two zymosan particles (yeast cell walls). Scale bar: 5 µm. Modified according to: Heinrich & Lee (2011).

The particle in the phagosome is destroyed by ROS and hydrolytic enzymes. During the oxidative burst, a large amount of superoxide anion radical is produced by NADPH oxidase (Kuwabara *et al.*, 2015). The superoxide anion radical is subsequently decomposed by superoxide dismutase (superoxide dismutase, SOD, EC 1.15.1.1) to hydrogen peroxide, which is decomposed by myeloperoxidase (myeloperoxidase, MPO, EC 1.11.2.2) to hypochlorous acid (Fig. 4) (Koyani *et al.*, 2015). This acid is also involved in the activation of proteases (Wang *et al.*, 2022).

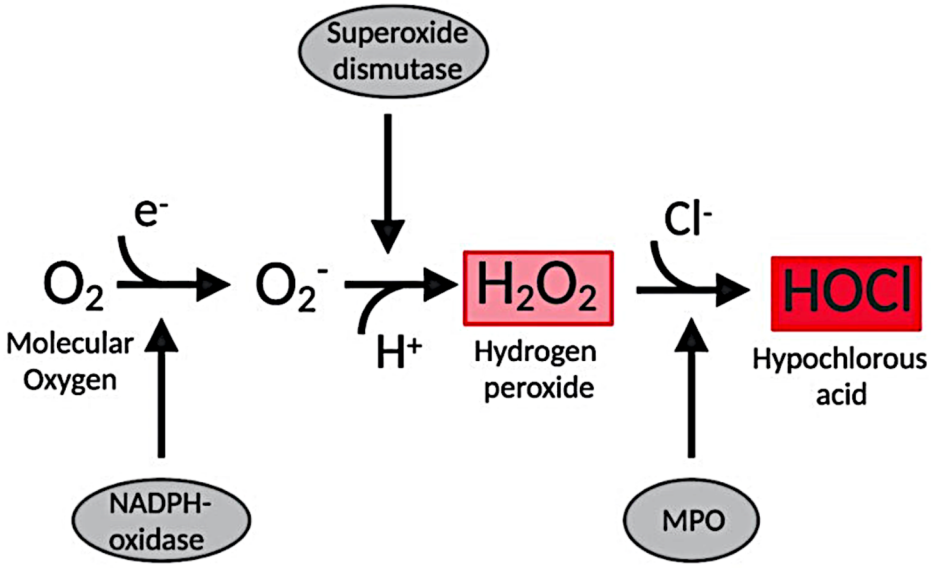

Figure 4. Schematic representation of neutrophil generation of hypochlorous acid. Adapted from: Nizer *et al.* (2020).

The mechanism of degranulation involves the deposition of neutrophil granules (see 2.1.2 Neutrophil granules) by exocytosis. As mentioned above, these granules contain antimicrobial substances that mediate pathogen elimination. Gelatinase (tertiary) granules are released first, followed by specific (secondary) granules, and then by the deposition of azurophilic (primary) granules (Yin & Heit, 2017). The sequential release of granules enables neutrophil migration and release of antimicrobial proteins at the site of infection. Granules with active substances are transported into phagosomes under normal conditions, demonstrating a direct connection between degranulation and phagocytosis (Klebanoff *et al.*, 2013).

2.2 Neutrophil extracellular traps

An alternative mechanism employed by neutrophils to combat invading pathogens is through the release of neutrophil extracellular traps (NETs). This process involves the formation of extracellular web-like structures (Fig. 5) composed of DNA (chromatin loosened from neutrophils) and proteins that are transported into the extracellular space. It has been shown that the DNA in NETs is primarily nuclear but may also originate from mitochondria. Since a large part of NETs is made of DNA, pathogens (mainly bacteria) expressing DNases can escape these traps (Halverson *et al.*, 2015). Proteins are delivered either from neutrophil granules (see 2.1.2 Neutrophil granules) or from the cytosol. In the case of cytosol proteins, this typically involves serine proteases (Majewski *et al.*, 2016). Histones may also participate in NETosis. Their acetylation has been shown to promote NETs formation (Hamam *et al.*, 2019).

Apart from eliminating pathogens, the NETs formation also serves as an effective physical barrier. This restrictive functionality is related to limiting the spread of pathogens, which is important for the treatment of diseases, such as sepsis (Castanheira & Kubes, 2019). A negative effect of NETs on the immune response has also been documented, wherein they prevented leukocytes from accessing tumour cells (Ireland & Oliver, 2020). NETosis has also received considerable attention in the context of the Coronavirus disease 2019 (COVID-19). A storm of pro-inflammatory cytokines has contributed to the acceleration of respiratory failure in many patients. These facts mentioned above demonstrate that NETs, besides their positive effects on the human immune system, can also cause health complications in some cases.

In terms of its progression, NETosis can be categorized as suicidal and vital. Suicidal NETosis is a type of cell death which involves the chromatin release and disruption of neutrophil granules allowing the mixing of nucleic acids with proteins from neutrophil granules (Vorobjeva & Pinegin, 2014). With perforation of the plasma membrane, NETs leak out of the cell that subsequently undergoes lysis. The suicidal NETosis is typical for PMA-stimulated neutrophils. The second option for neutrophils is to perform viable NETosis without cell lysis (Pieterse *et al.*, 2016). Vital NETosis of neutrophils can be induced by LPS (Ding *et al.*, 2021). A striking contrast between these two types of NETs formation is the duration. In the case of suicidal NETosis, formed NETs remain active for hours. Vital NETosis, however, can last for as little as 30 min (Byrd *et al.*, 2013). As the name suggests, vital NETosis is performed by intact neutrophils and does not limit their further functionality.

Besides the above-mentioned positive effects on the human immune system, the formation of NETs can lead to negative consequences. In 2010, Hakkim *et al.* reported a mechanism connecting impaired NETs degradation and glomerulonephritis in systemic lupus erythematosus (an autoimmune disease). The effect of NETs on thrombosis development was also observed (Savchenko *et al.*, 2014). Excessive NETs formation has also been linked with organ damage, e.g. during influenza pneumonitis (Porto & Stein, 2016).

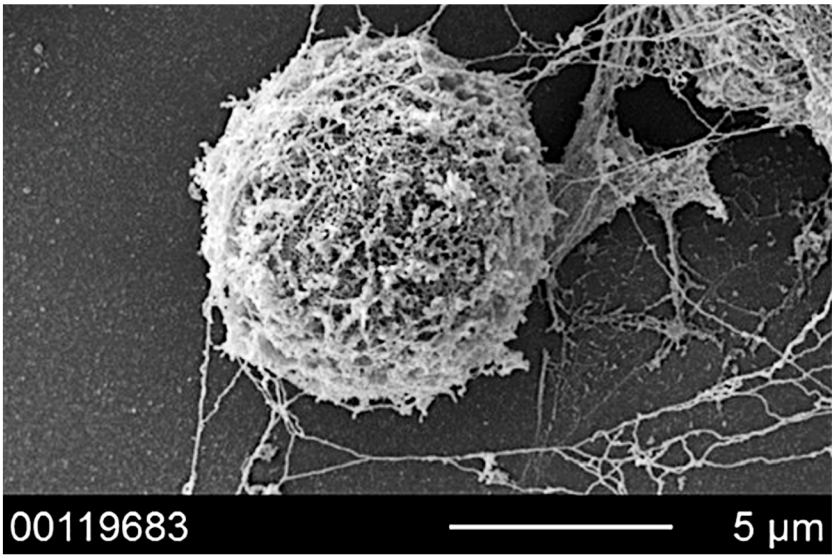

Figure 5. Formation of NETs by a human neutrophil (SEM image). Scale bar: 5 µm. Modified according to: Giaglis *et al.* (2016).

2.3 Reactive oxygen species

The term reactive oxygen species (ROS) includes oxygen radicals and non-radical molecules. Radicals are the following: superoxide ion radical ($O_2^{\bullet -}$), hydroxyl radical ($HO^{\bullet}$), peroxyl radical ($ROO^{\bullet}$), and hydroperoxyl radical ($HO_2^{\bullet}$). Non-radical molecules include hydrogen peroxide (H_2O_2), hypochlorous acid (HOCl), ozone (O_3) or singlet oxygen ($^1O_2$). ROS are primarily formed from the diatomic oxygen molecule (O_2) by its reduction (Fig. 6) – commonly as byproducts in living systems. The properties of these molecules (mainly radicals) make them highly reactive (Dumanović *et al.*, 2021).

ROS are commonly present in low concentrations in cells and play an essential role in cell signalling and homeostasis (Redza-Dutordoir & Averill-Bates, 2016). However, high concentrations of ROS cause problems for cells that are often incompatible with normal functioning (Schieber & Chandel, 2014).

ROS formation can be classified into enzymatic and non-enzymatic. The enzymatic pathway involves many metabolic processes – mainly the mitochondrial respiratory chain (Stefanatos & Sanz, 2018), NADPH oxidase activity during phagocytosis (as mentioned above) or cytochrome P450 (cytochrome P450, CYP, 1.14.14.1), which is essential for the detoxification of xenobiotics (McDonnell & Dang, 2013). In the case of plant cells, photosynthesis represents an important source of ROS (Pospíšil, 2016).

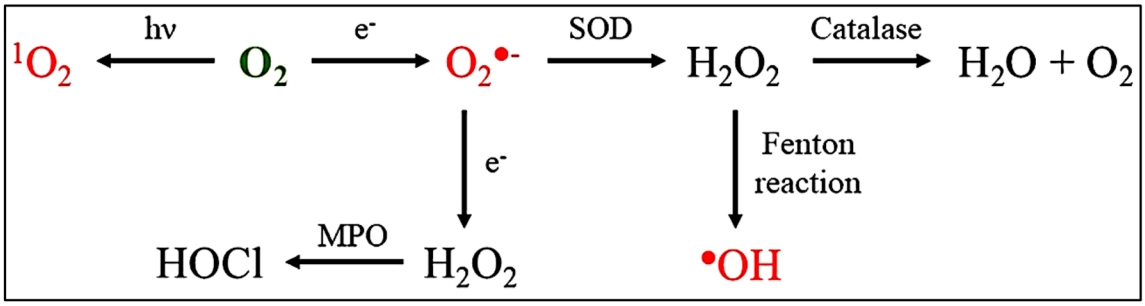

Figure 6. Formation of radical and non-radical ROS – diatomic oxygen reduction. Adapted from: Čapek & Roušar (2021).

Since ROS cause oxidative damage to cells, it is necessary to maintain an acceptable level of ROS in the cell. For this purpose, systems of antioxidants have been developed in living systems. The most important enzymatic antioxidants are superoxide dismutase (catalysing the conversion of the superoxide anion radical into hydrogen peroxide), catalase (catalysing the conversion of hydrogen peroxide into water and oxygen) or glutathione peroxidase (glutathione peroxidase, GPx, EC 1.11.1.9) which catalyses the conversion of hydrogen peroxide into water. Important non-enzymatic antioxidants include vitamins, such as ascorbic acid or tocopherol (Mirończuk-Chodakowska *et al.*, 2018).

It has been found that the overproduction of ROS in the human body can promote the development of various diseases including cardiovascular disorders (Moris *et al.*, 2017), cognitive impairment (Hernandes *et al.*, 2014) or cancer (Galadari *et al.*, 2017). Oxidative stress caused by excessive ROS damages biomacromolecules which includes oxidation of nucleic acids (DNA, RNA), amino acids in proteins, cofactors (leading to enzyme deactivation), and last but not least, lipid peroxidation – oxidation of polyunsaturated fatty acids (Juan *et al.*, 2021).

2.3.1 Involvement of reactive oxygen species in NETosis

Numerous scientific articles published in recent years have demonstrated that ROS are essential for NETosis activation. However, the specific mechanism is yet to be discovered (Douda *et al.*, 2015). One possible pathway of NETosis initiation is the ROS-mediated activation of transcription factors. A clear interaction with ROS has been observed in the case of transcription factors hypoxia-inducible factor-1 (HIF-1) and nuclear factor kappa B (NF-κB). These transcription factors are reported to regulate the gene expression of proteins that are crucial for NETosis (Zhong *et al.*, 2022). Further research has revealed that the transcription factor NF-κB regulates the level of ROS in cells, and vice versa, ROS also affect the activity of this transcription factor (Hoesel & Schmid, 2013).

ROS may also regulate the activity of enzymes that are critical for the formation of NETs (Stoiber *et al.*, 2015). Cytokines like IL-8 are known to regulate ROS levels within cells as well as to trigger NETosis (Gupta *et al.*, 2014; Zha *et al.*, 2020).

2.3.2 Lipid peroxidation, reactive oxygen species and NETosis

As mentioned above, an increase in the level of ROS or free radicals can impose direct damage on lipids. Free radicals can oxidise membrane phospholipids resulting in the formation of lipid hydroperoxides and aldehydes as primary and secondary products, respectively. Lipid peroxidation events can damage the structure and integrity of membranes (van der Paal *et al.*, 2015; Zhong *et al.*, 2019). Among the secondary aldehyde products, malondialdehyde (MDA), 4-hydroxynonenal (4-HNE), propanal and hexanal are widely studied (Ayala *et al.*, 2014). MDA is the final product of arachidonic acid degradation. MDA can be produced in the body by enzymatic and non-enzymatic pathways. MDA molecules are also able to interact with biomacromolecules (proteins, nucleic acids) and form adducts (Zarkovic *et al.*, 2013). MDA binds to amino groups of amino acids (mainly lysine) in proteins (Fig. 7) to form MDA epitopes (Papac-Milicevic *et al.*, 2016). Measurement of total MDA by high-performance liquid chromatography (HPLC) or detection of MDA-derived protein adducts using antibodies can aid in deciphering its role in disease pathogenesis (Bézière *et al.*, 2014; Manoharan *et al.*, 2023). Oxidised phospholipids are known to modulate the function of leukocytes and play a critical role in the extracellular traps formation in neutrophils.

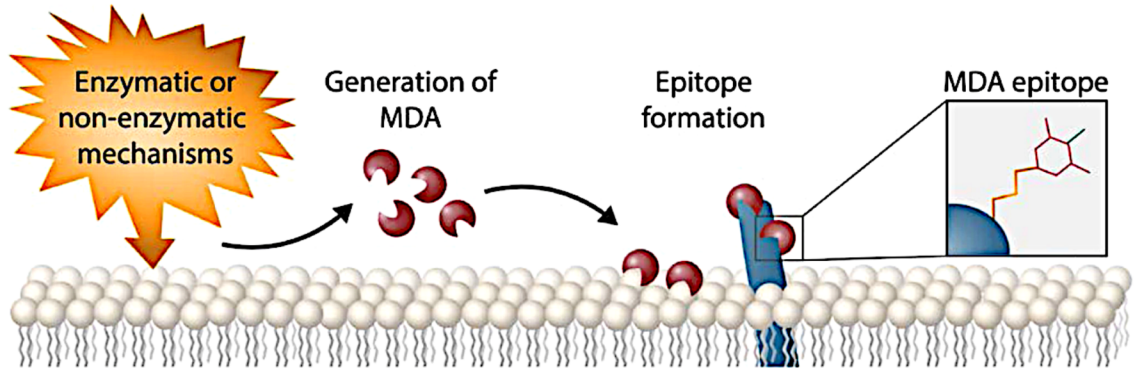

Figure 7. Lipid peroxidation of fatty acids resulting in formation of MDA. Molecules of MDA bind to amino groups of amino acids and form MDA epitopes. Adapted from: Papac-Milicevic *et al.* (2016).

2.4 HL-60 cell line

HL-60 is a human promyelocytic leukemia cell line originally isolated from the bone marrow of a 36-year-old woman with acute promyelocytic leukemia in 1977. With inducers, these cells can be differentiated into either neutrophils or monocytes/macrophages-like cells *in vitro* (Ramachandran *et al*., 2014). This cell line, which is growing in popularity, is often used in laboratory research due to its beneficial characteristics. HL-60 cells continuously proliferate in cell suspensions, with a doubling time of approximately 36–48 h. The presence of transferrin and insulin is essential for cell division (McTague *et al*., 2022). In culture, cells resemble an ovoid or a spherical (Fig. 8A) shape, and the surface is smooth in the undifferentiated state (Shirai *et al*., 2018). These cells are heterogenous in size with a diameter of approximately 10–20 μm, depending on the growth conditions (Chen *et al*., 2016). HL-60 cells are also characterized by the presence of azurophilic granules (Razvina *et al*., 2015). The nucleus of the cell is usually large and round (Fig. 8B).

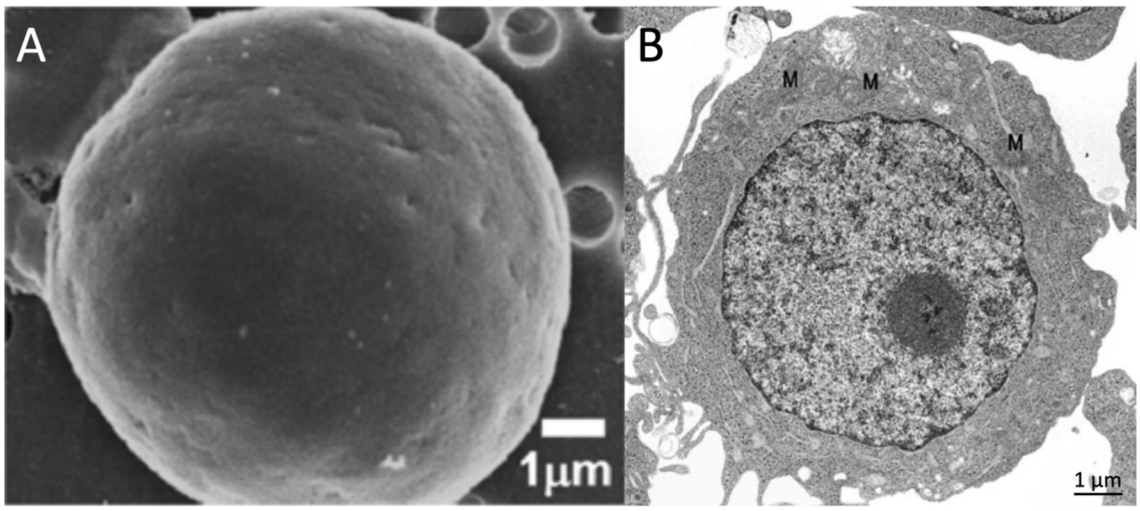

Figure 8. Morphology of HL-60 cells. **(A)** SEM image of an HL-60 cell. **(B)** TEM image of an HL-60 cell with a round nucleus, nucleolus and mitochondria **(M)**. Scale bars: 1 μm (both images). Modified according to: **(A)** Zhong *et al*. (2011), **(B)** Salvioli *et al*. (2003).

2.4.1 HL-60 cells differentiation and utilization

The HL-60 cell line has drawn the attention of researchers due to its ability to differentiate into different cell types under *in vitro* conditions. Due to this advantageous property, the HL-60 cell line, together with the U-937 and THP-1 cell lines, is used as an *in vitro* model for the study of the cell differentiation (Nascimento *et al.*, 2022).

The discoverer of the HL-60 cell line, Steven J. Collins, observed that these cells can differentiate into four cell types (Fig. 9): granulocytes (neutrophils, eosinophils), monocytes, and macrophage-like cells (Collins, 1987). The cell type that the HL-60 cell will differentiate into depends on the inducing agent. Most commonly, HL-60 cells differentiate into neutrophils, which may be induced by the use of agents dimethyl sulfoxide (DMSO) or retinoic acid (Babatunde *et al.*, 2021). The differentiation into neutrophils is associated with a change in the cell shape. Cell extensions and the formation of pseudopodia occur, as can be observed in the study of Wang *et al.* (2017). Eosinophil formation was observed upon stimulation with granulocyte-macrophage colony-stimulating factor (GM-CSF). However, this represented only a small percentage (4–7%) of the total number of differentiated cells (Fu *et al.*, 2016). Differentiation of HL-60 cells into monocytes can be induced by several stimuli, e.g. vitamin D_3 (Poplutz *et al.*, 2014). To differentiate HL-60 cells into macrophage-like cells, phorbol-12-myristate-13-acetate (PMA) is standardly employed.

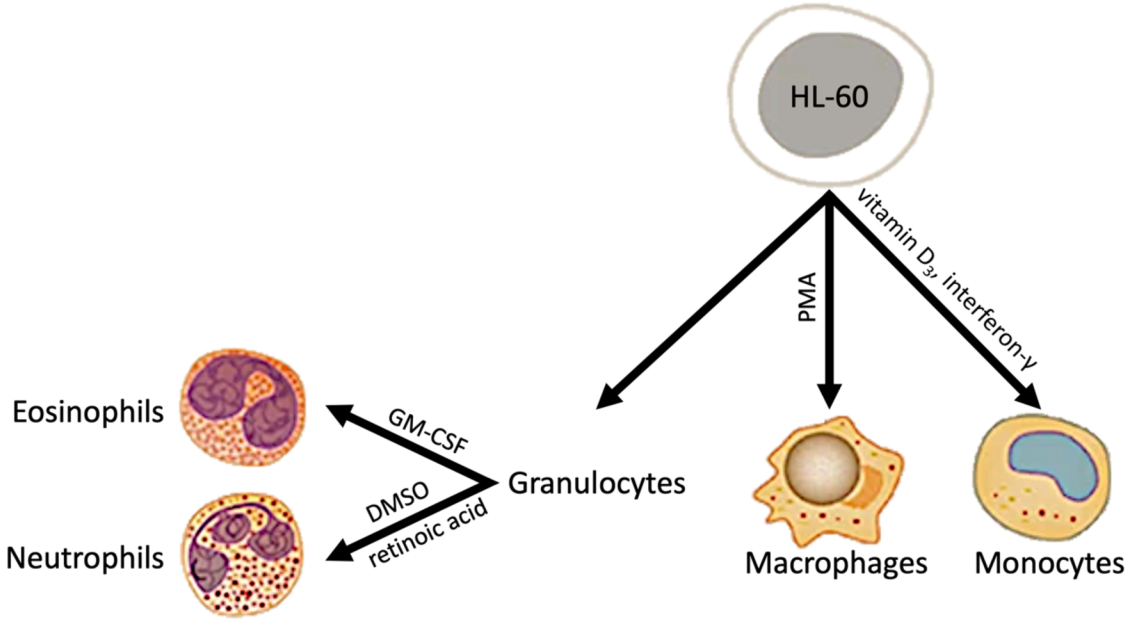

Figure 9. Differentiation of HL-60 cells into different cell types: granulocytes (neutrophils, eosinophils), monocytes, and macrophage-like cells. Modified according to: Hou *et al.* (2020).

However, the cellular responses of these cells differ from non-leukaemic cells, which represents a relevant limitation of these *in vitro* models (Nascimento *et al.*, 2022).

HL-60 was utilized as a promising *in vitro* model to study various cellular processes like cell death processes (Huang *et al.*, 2019), and analysis of macrophage functions – e.g. phagocytosis (Mandic *et al.*, 2022). It is also employed in the investigation of immune responses following infection by a pathogen (Lee *et al.*, 2017) or the development of new drugs against various diseases, including leukaemia or cancer (Shaikh *et al.*, 2014).

2.5 Exploring the biotechnological potential of NETosis

Many recent studies indicating that NETs are connected to several biological processes which may hold potential for novel biotechnological applications have frequently been focused on NETosis.

The first use of neutrophil extracellular traps in medical biotechnology is disease diagnostics. NETs contain proteins that can be used as biomarkers to identify diseases. Numerous studies have established a link between elevated NETs levels and the development of COVID-19, which may be used for diagnostic purposes (Zuo *et al.*, 2020; Blanch-Ruiz *et al.*, 2022).

Another field of medical biotechnology application of NETs is cancer therapy. Many hypotheses support the anti-cancer effect of NETs through the direct killing of cancer cells or stimulation of immune responses. However, this fact is yet to be confirmed and remains shrouded in uncertainty. Besides, studies have also demonstrated the pro-cancer effect of NETs wherein they provide a suitable environment for metastasis (Cools-Lartigue *et al.*, 2014; Garley *et al.*, 2016).

While describing medical biotechnology applications, it is essential to mention the treatment of autoimmune diseases. Particular attention is focused on the NETs inactivation during rheumatoid arthritis (RA) which is characterized by joint inflammation and bone damage. NETs displace autoantigens, such as citrullinated histones, which enhance immune responses to RA (Fousert *et al.*, 2020). Histone citrullination (an epigenetic post-translational modification during which histone arginine is converted to citrulline) occurs during NETs formation (Tsourouktsoglou *et al.*, 2020).

Last but not least, an interesting application of nanomedical biotechnology is the neutrophil-based drug delivery system (Fig. 10). This method can provide an innovative and efficient approach in which therapeutic agents are packaged into nanoparticles that are subsequently attached to activated neutrophils using specific ligands (Wang *et al.*,

2021; Cruz *et al*., 2022). However, the approach demands further research and is still under development (Chu *et al*., 2018).

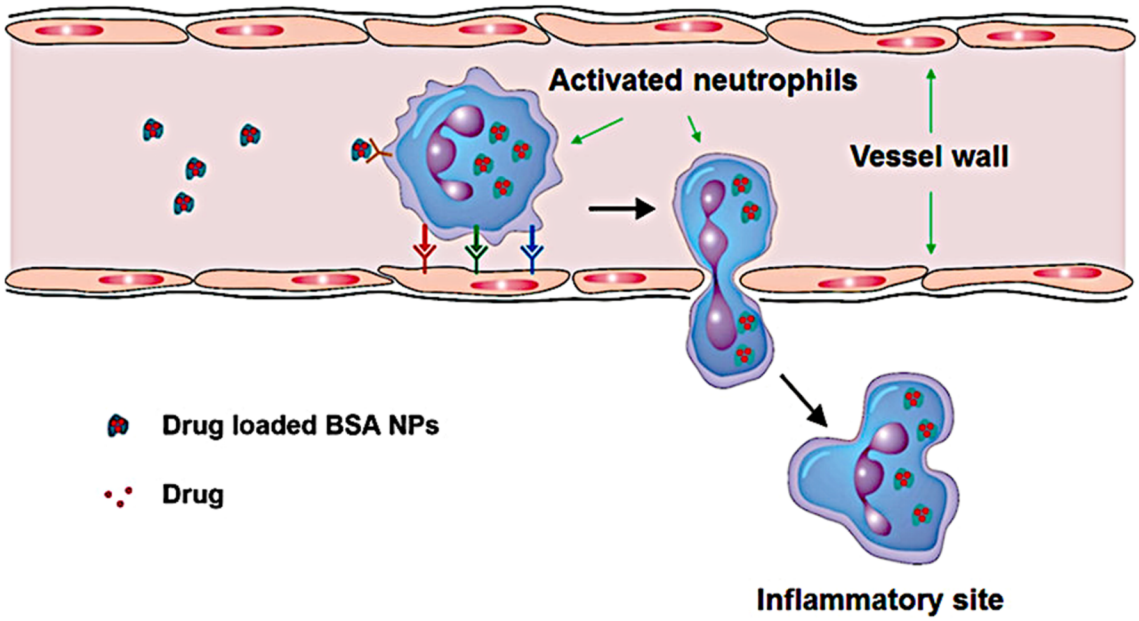

Figure 10. Scheme of the neutrophil-based drug delivery system. Drug loaded bovine serum albumin **(BSA)** nanoparticles **(NPs)** are attached to activated neutrophils using specific ligands. Activated neutrophils with NPs are transported via blood vessels and, if necessary, cross the vessel wall to reach the site of inflammation. Modified according to: Chu *et al*. (2015).

2.6 Characterization of methods for detecting superoxide anion radical and malondialdehyde protein adducts

2.6.1 Electron paramagnetic resonance spin trapping: Superoxide anion radical detection

The detection of superoxide anion radical (and other ROS) is accompanied by difficulties arising from the instability of these molecules and their short lifetime. Identification of ROS molecules can also be negatively affected by the limited amounts in which they are generated. This places demands on the higher sensitivity of the methods applied. However, these limitations can be successfully overcome by electron paramagnetic resonance (EPR) spin trapping (Abbas *et al.*, 2016).

EPR is an analytical method investigating the behaviour of molecules with unpaired electrons in samples. Applying magnetic fields to the sample results in the transition of unpaired electrons between two spin states. The change in energy (characteristic for each radical) is subsequently detected (Roessler & Salvadori, 2018).

For the detection of radical ROS, it is preferable to use the spin-trapping technique. This elegantly solves the complications of the instability and short lifetime of these molecules. ROS molecules covalently react with the spin trap to form stable spin-labelled adducts, which are subsequently identified by EPR spectroscopy (Davies, 2016).

2.6.2 Detecting malondialdehyde protein adducts using western blotting: A reliable and sensitive approach

As mentioned above, the analysis of MDA-protein adducts is utilized as a marker of oxidative protein damage. MDA-protein adducts can be efficiently detected by SDS-PAGE followed by western blotting.

The technique involves electrophoretic separation of extracted proteins (including MDA-protein adducts) by standard SDS-PAGE based on their molecular weight. The separated proteins are then transferred onto the nitrocellulose membrane and specific protein detection is achieved by the use of an anti-MDA primary antibody. Species-specific HRP-labelled secondary antibodies recognize and bind to primary antibodies allowing chemiluminescence detection of targeted proteins (Liao *et al.*, 2018).

Similar to all analytical methods, this MDA-protein adduct detection has its pros and cons. Advantages include sensitivity, specificity or the ability to analyse multiple samples simultaneously. Disadvantages are, among others, false positive results, the cost of specific antibodies or their poor quality (Gilda *et al.*, 2015).

3 MATERIALS AND METHODS

3.1 Reagents, media and antibodies

HL-60 cell lines were procured from American Type Culture Collection (ATCC; Rockville, MD, USA) and cultured in RPMI 1640 media (LM-R1639) supplemented with 10% fetal bovine serum (FBS), 1% (*v/v*) antibiotic-antimycotic solution from Biosera (Nuaille, France). All-trans retinoic acid (R2625-500MG) was obtained from Merck – Sigma-Aldrich® (Burlington, MA, USA). Phorbol-12-myristate-13-acetate (P1585) was procured from Merck – Sigma-Aldrich® (Burlington, MA, USA). Lipopolysaccharides (L2630) were obtained from Merck – Sigma-Aldrich® (Burlington, MA, USA). 2-ethoxycarbonyl-2-methyl-3,4-dihydro-2*H*-pyrrole-1-oxide (No. ALX-430-098) was purchased from Enzo Life Science (Farmingdale, NY, USA). A Pierce™ BCA Protein Assay Kit (No. 23227) was procured from Thermo Fisher Scientific (Waltham, MA, USA). A Pierce™ Bovine Serum Albumin Standard Pre-Diluted Set (No. 23208) was also purchased from Thermo Fisher Scientific (Waltham, MA, USA). An MTT Assay Kit (ab211091) was obtained from Abcam (Cambridge, CB2 0AX, UK). The Immobilon® Western Chemiluminescent HRP Substrate (WBKLS0500) was procured from Merck – Millipore® (Burlington, MA, USA). The primary rabbit IgG anti-MDA antibody (ab27642) was obtained from Abcam (Cambridge, CB2 0AX, UK). The secondary goat anti-rabbit IgG (H+L) HRP conjugate (No. 1721019) was purchased from Bio-Rad (Hercules, CA, USA). Complete Protease inhibitors cocktail tablets (No. 4693159001) were obtained from Roche (Mannheim, Germany). FM4-64 stain (T13320) was procured from Merck – Sigma-Aldrich® (Burlington, MA, USA) and Hoechst 33342 stain (No. 62249) was purchased from Thermo Fisher Scientific (Waltham, MA, USA).

3.2 Cell viability assay

The cell viability of HL-60 cells was determined using an MTT Assay Kit. Cells were treated with varying concentrations of stimulants (PMA, ATRA, LPS) and post-treatment cell viability and proliferation abilities were established. HL-60 cells (1×10^6 cells·mL^{-1}) were cultured in a 96-well plate at 37 °C and 5% CO_2. Cells were treated with different concentrations of PMA (500–18.75 nmol·L^{-1}), LPS (1,000–37.5 ng·mL^{-1}) and ATRA (3–0.09 μmol·L^{-1}) for 24 h (PMA, LPS) and 72 h – ATRA, respectively (Fig. 11). Post incubation, the treatment media was carefully removed from the wells and replaced with 50 μL of the serum-free RPMI 1640 media and 50 μL of the MTT Reagent in each well. Followed by incubation for 3 h (37 °C, 5% CO_2), 150 μL of the MTT Solvent was added

into each well (Fig. 12) and incubated for 15 min. on an orbital shaker. The absorbances were measured at 590 nm using a Synergy™ Mx Microplate Reader (BioTek Instruments; Winooski, VT, USA). Measurements for each agent concentration were performed in duplicates. Based on these results, optimal concentrations of PMA, ATRA and LPS were selected and subsequently used in our following experiments. Sufficient differentiation of HL-60 cells had to be considered, but at the same time, the chosen concentrations of the agents must not be too cytotoxic for the cells.

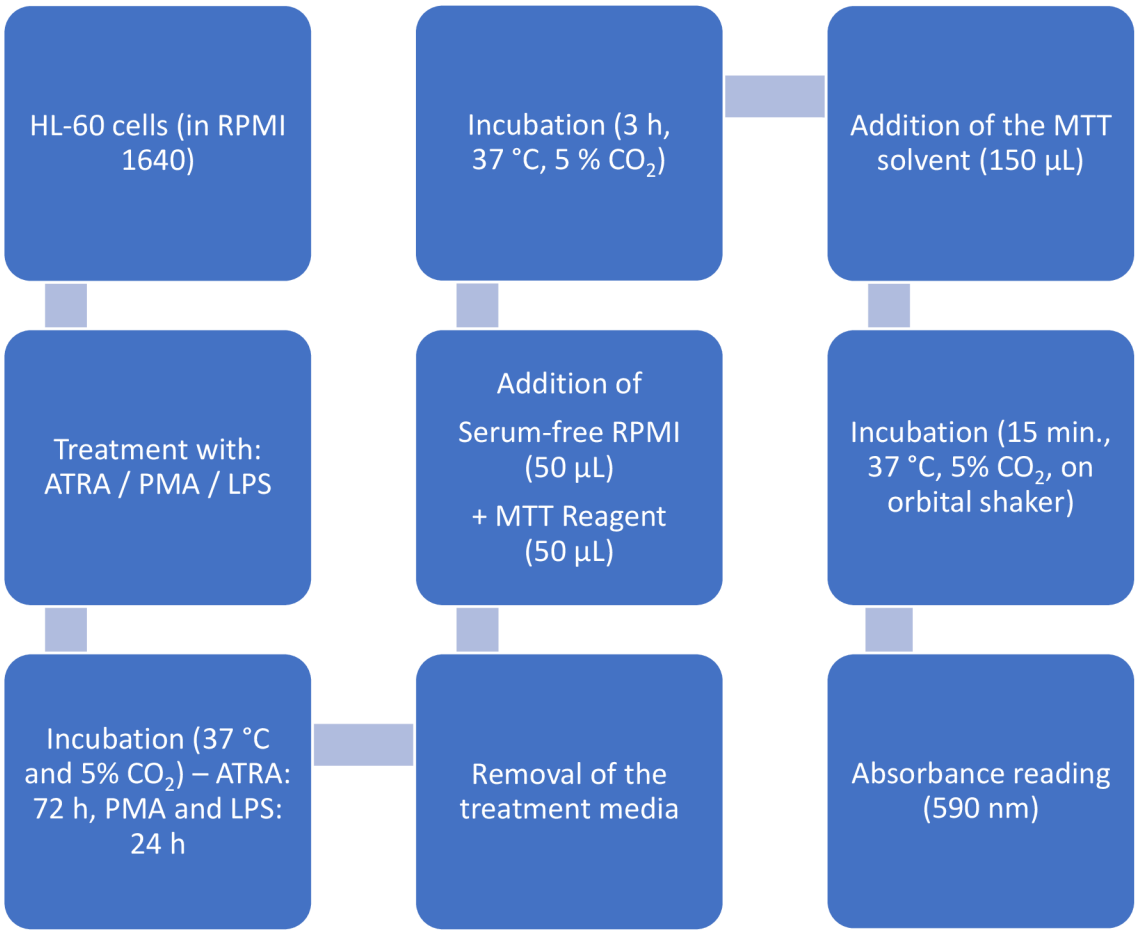

Figure 11. Schematic illustration of the Cell viability assay workflow.

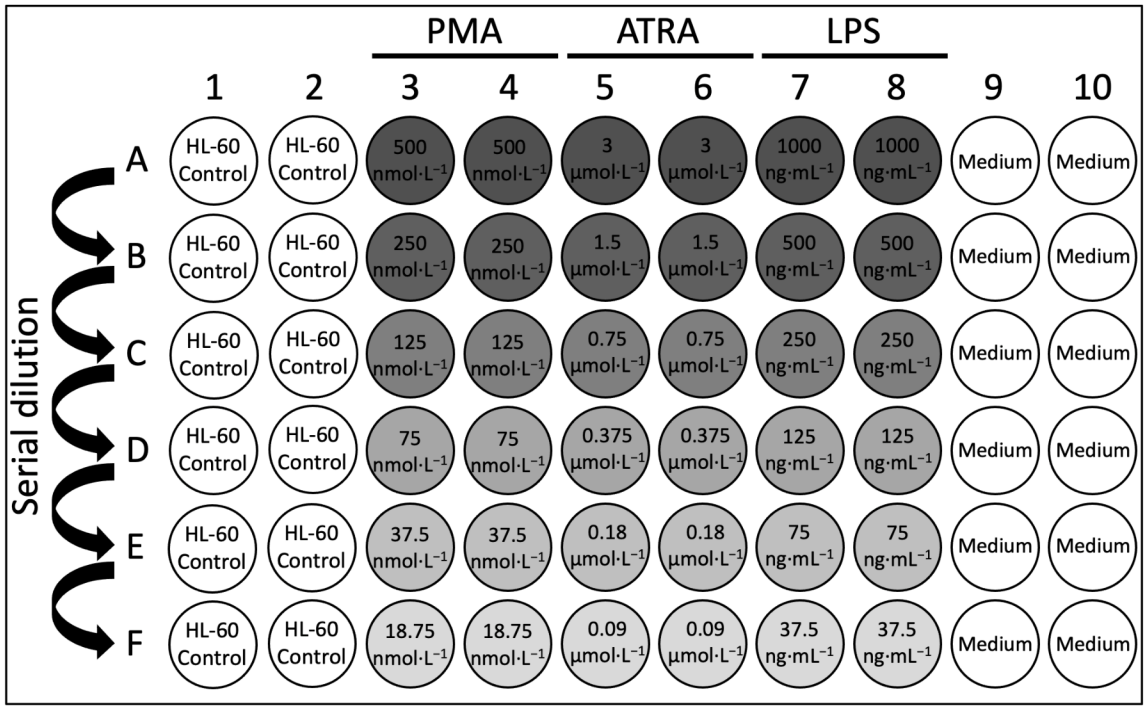

Figure 12. Schematic illustration of the serial dilution of differentiating agents for Cell viability assay.

3.3 Cell culture and differentiation

HL-60 cells were cultured in the RPMI 1640 cell culture medium. Fetal bovine serum (10%), antibiotics (penicillin/streptomycin, 1% *v/v*) and L-glutamine (0.3 $g \cdot L^{-1}$) were added to the medium. The cells were cultured in a MITRE 4000 Series culture incubator (Contherm; Lower Hutt, New Zealand) under constant temperature (37 °C) and CO_2 concentration in the atmosphere (5%).

The main aim of our research was the HL-60 cell differentiation into neutrophils using ATRA and the following neutrophil activation using PMA and LPS (Fig. 13) to study the free radical generation and protein adducts formation.

For our experiments, the HL-60 cells were differentiated into neutrophils using ATRA (0.25 $\mu mol \cdot L^{-1}$, incubation for 72 h) in the complete RPMI medium. The subsequent neutrophil activation was achieved using PMA (50 $nmol \cdot L^{-1}$) or LPS (100 $ng \cdot mL^{-1}$). Concentrations used in our differentiation and activation studies were selected based on the Cell viability assay (see 3.2. Cell viability assay). Differences in cellular morphology along the differentiation process were monitored by confocal laser scanning microscopy (see 3.5. Confocal laser scanning microscopy). The neutrophil activation (PMA, LPS) was carried out for a period of 3 h in the serum-free RPMI medium.

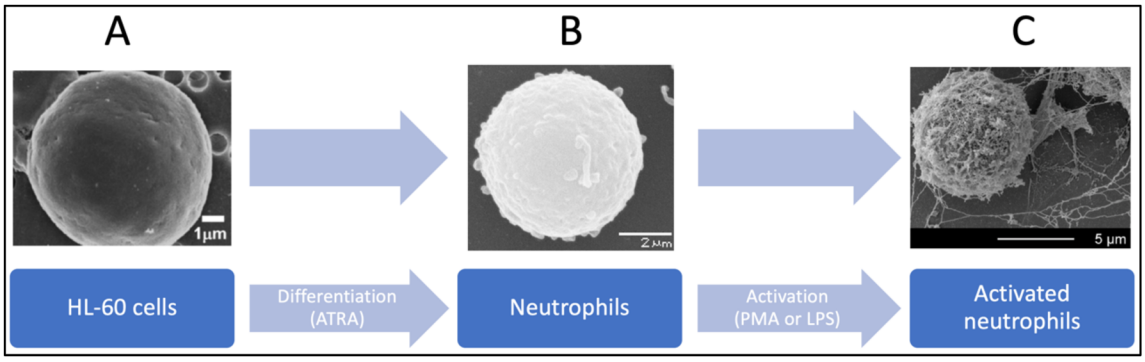

Figure 13. Scheme of the differentiation of HL-60 cells into neutrophils and the following neutrophil activation. **(A)** SEM image of an HL-60 cell. Scale bar: 1 µm. **(B)** SEM image of a neutrophile. Scale bar: 2 µm. **(C)** SEM image of the activated neutrophile and NETosis. Scale bar: 5 µm. Modified according to: **(A)** Zhong *et al.* (2011), **(B)** Lázaro-Díez *et al.* (2020), **(C)** Giaglis *et al.* (2016).

Washing of HL-60 cells was done with phosphate buffer saline (PBS; pH 7.4) to remove residual culture media. Cell density was quantified using the TC20 Automated Cell Counter (Bio-Rad; Hercules, CA, USA) by staining cells with trypan blue (T6146; Merck – Sigma-Aldrich®; Burlington, MA, USA).

3.4 Superoxide anion radical detection using electron paramagnetic resonance spin trapping spectroscopy

Production of superoxide anion radical ($O_2^{\bullet-}$) during the HL-60 differentiation was monitored using an EPR spectrometer MiniScope MS400 (Magnettech GmbH; Berlin, Germany). HL-60 cells were differentiated as mentioned in section 3.3. Control undifferentiated samples and treated samples were collected by centrifugation (Centrifuge 5425 R; Eppendorf; Hamburg, Germany) at ~ 394 × g for 10 min. at room temperature (RT). The resulting cell pellets were washed in PBS buffer (0.1 mol·L^{-1}) through centrifugation (~ 394 × g, 10 min., RT) and the process was repeated twice to remove residual media. Treated pellets were resuspended in PBS and incubated along with 2-ethoxycarbonyl-2-methyl-3,4-dihydro-2*H*-pyrrole-1-oxide (EMPO; 25 mmol·L^{-1}) for 15 min. at 37 °C. (Fig. 14). The reaction mixture was transferred into a glass capillary tube and subjected to the EPR analysis. The data were recorded using the following parameters (Prasad *et al.*, 2021): modulation frequency (100 kHz), microwave power (10 mW), sweep width (100 G), modulation amplitude (1 G), and scan rate (1.62 G·s^{-1}). Undifferentiated HL-60 cells in PBS were used as a control sample.

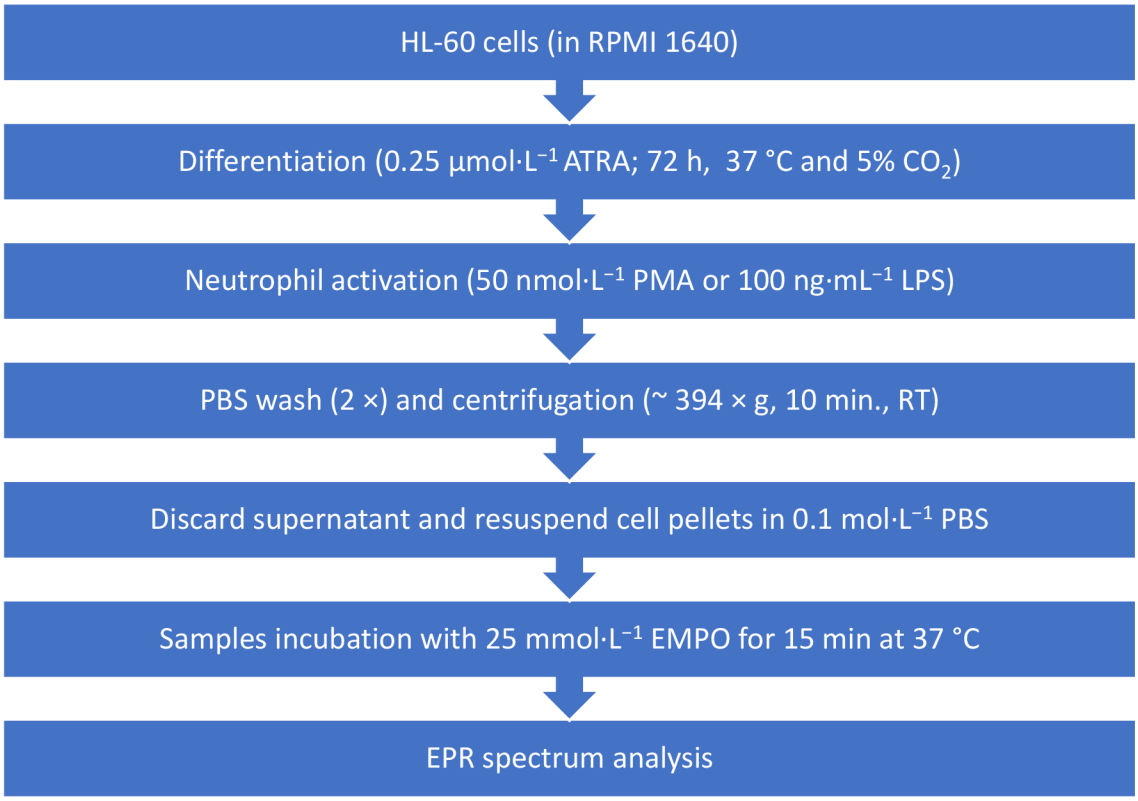

Figure 14. Scheme of the EPR spectroscopy workflow.

3.5 Confocal laser scanning microscopy

Membrane integrity, morphological changes, and generation of reactive oxygen species in differentiating HL-60 cells were observed using confocal laser scanning microscopy (CLSM).

Undifferentiated cells were used as a control. As mentioned above, HL-60 cells were differentiated and activated with respective stimuli. Post treatment, cells were collected by centrifugation (~ 394 × g, 10 min., RT) and resulting pellets were resuspended in 100 µL of fresh serum-free media. Cell suspensions were incubated with plasma membrane-specific dye FM4-64 (15 µmol·L^{-1}) and nucleic acid-specific dye Hoechst 33342 (2 µmol·L^{-1}) for 5 min. to observe the integrity of membranes and nuclei. Visualization was performed using a Fluorview 1000 confocal unit attached to an IX80 microscope (Olympus Czech Group; Prague, Czech Republic). Excitation was done using a 543 nm He-Ne laser and a 655–755 nm emission filter. Morphologies of the cells with lower contrasts were visualized in CLSM using a transmitted light detection module with a 405 nm diode laser excitation and Nomarski – differential interference contrast (DIC) filters (Fig. 15).

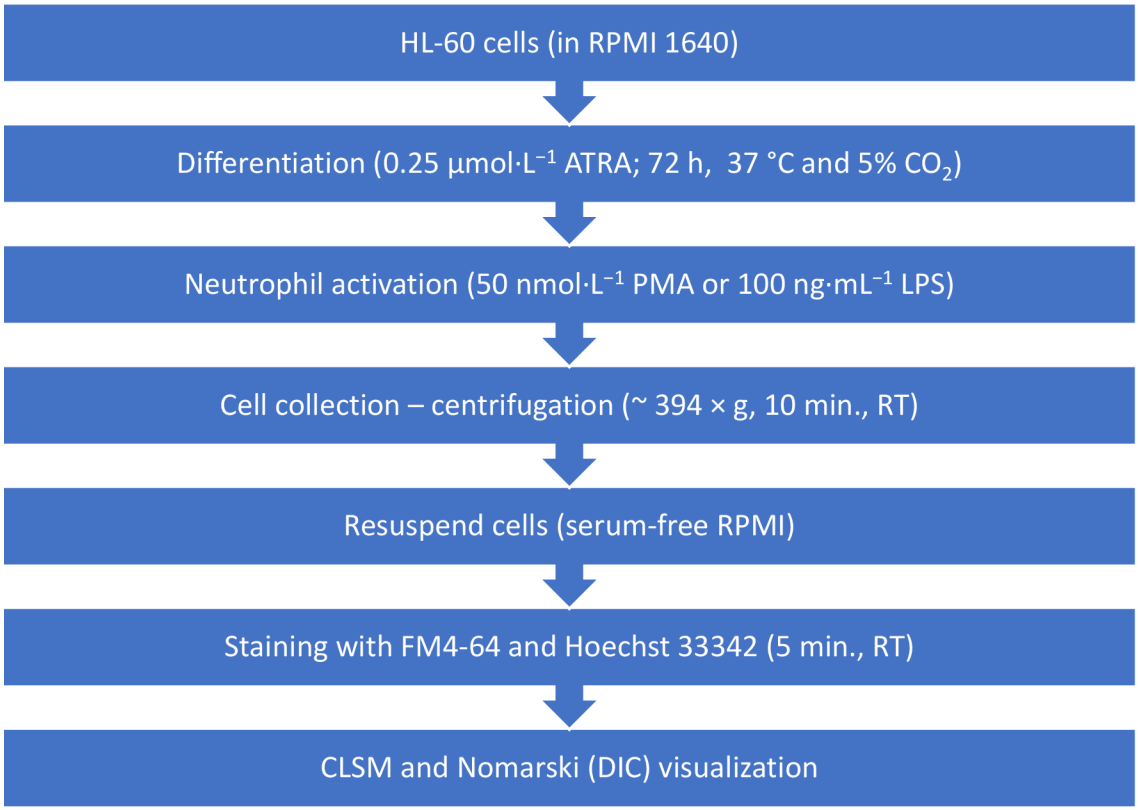

Figure 15. Scheme of the CLSM workflow.

3.6 Cell lysis and whole cell protein extraction

HL-60 cells were differentiated into neutrophils and the neutrophils were subsequently activated (see 3.3. Cell culture and differentiation). After the centrifugation (~ 394 × g, 10 min., RT) and the media removal, the cells were washed twice with PBS buffer (~ 394 × g, 10 min., RT). After the PBS removal, the cell pellets were resuspended in 100 µL of lysis buffer (radioimmunoprecipitation assay – RIPA – buffer). RIPA buffer: 150 mmol·L^{-1} NaCl, 50 mmol·L^{-1} Tris-(hydroxyethyl)-aminomethane – Tris (for 1 L: 200 mmol·L^{-1} Tris salts, 1.5 mol·L^{-1} NaCl, distilled water), 0.5% sodium deoxycholate, 1% nonyl phenoxypolyethoxylethanol – NP-40, 1% *v*/*v* protease inhibitor cocktail. All samples (Tab. 1) went through sonication: 6 cycles, 20 s on and 10 s off (in the ice), 3 min. in total. The resulting mixture was centrifuged (~ 19,318 × g, 30 min., 4 °C). After the centrifugation, the supernatant was collected into tubes (Fig. 16).

Table 1. Samples used for the protein analysis.

Sample number	Sample	Protein concentration used [$\mu g \cdot mL^{-1}$]
1	Undifferentiated control	20
2	0.25 $\mu mol \cdot L^{-1}$ ATRA differentiated control	20
3	0.25 $\mu mol \cdot L^{-1}$ ATRA + 50 $nmol \cdot L^{-1}$ PMA (1.5 h)	20
4	0.25 $\mu mol \cdot L^{-1}$ ATRA + 50 $nmol \cdot L^{-1}$ PMA (3 h)	20
5	0.25 $\mu mol \cdot L^{-1}$ ATRA + 100 $ng \cdot mL^{-1}$ LPS (1.5 h)	20
6	0.25 $\mu mol \cdot L^{-1}$ ATRA + 100 $ng \cdot mL^{-1}$ LPS (3 h)	20

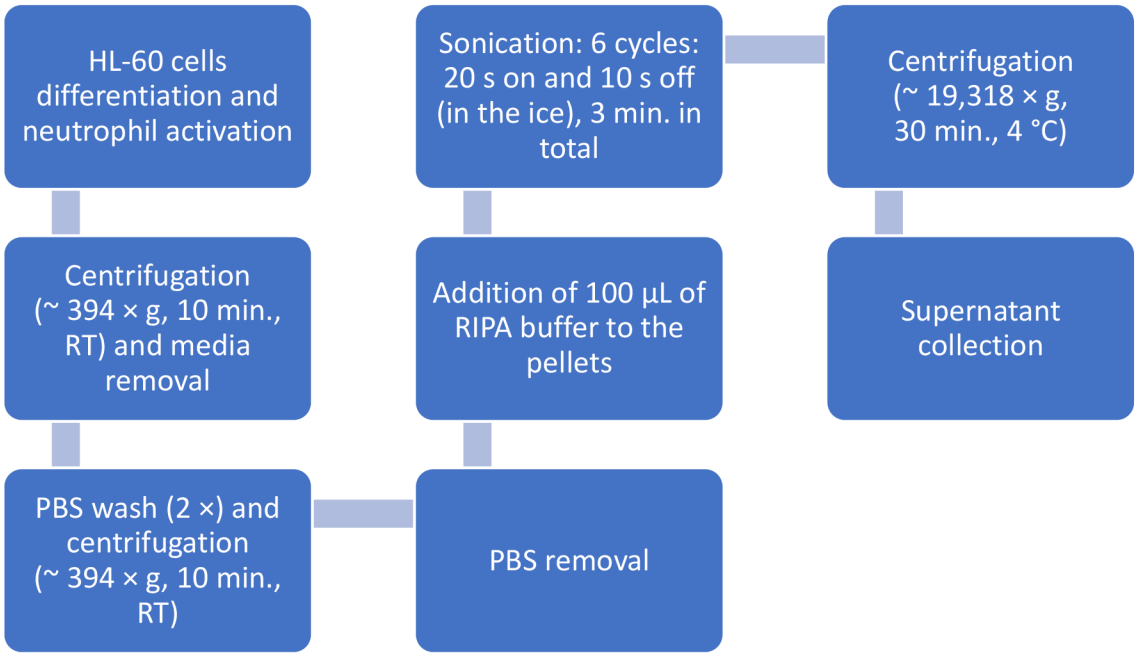

Figure 16. Scheme of the protein extraction workflow.

3.7 Protein quantification

Bovine serum albumin (BSA) pre-diluted set (Tab. 2; 10 µL) from Thermo Fisher Scientific was used as reference standards for generating a standard curve and a calibration control in this BCA protein assay. Seven different concentrations of BSA standards, whole cell protein supernatants (Tab. 3; 2.5 µL), and two control blank samples (RIPA buffer; 10 µL) were transferred onto a 96-well plate. Furthermore, 200 µL of the working reagent was added to each used well (the working solution was prepared by mixing Reagent A and Reagent B in a ratio of 50:1). The absorbance was measured at 562 nm using the Synergy™ Mx Microplate Reader, post incubation for 30 min at 37 °C. The average absorbance value of the blank samples was subtracted from the average absorbance values of all standards and samples. A standard BSA curve (Fig. 17) was prepared by plotting the average absorbance value of each BSA standard vs. its concentration [µg·mL^{-1}] using Microsoft Excel. The standard curve was used for the calculation of the protein concentrations of the samples (Fig. 18).

Table 2. BSA standard concentrations and volumes.

BSA standard concentration [µg·mL^{-1}]	Volume [µL]
125	10
250	10
500	10
750	10
1,000	10
1,500	10
2,000	10

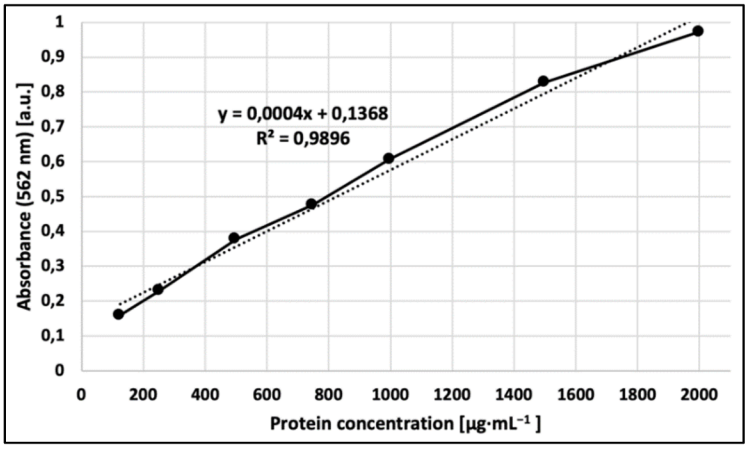

Figure 17. The standard BSA curve prepared from the BSA standards average absorbance values.

Table 3. Protein quantification samples and volumes.

No.	Sample	Volume [µL]
1	Undifferentiated control	2.5
2	0.25 µmol·L^{-1} ATRA differentiated control	2.5
3	0.25 µmol·L^{-1} ATRA + 50 nmol·L^{-1} PMA (1.5 h)	2.5
4	0.25 µmol·L^{-1} ATRA + 50 nmol·L^{-1} PMA (3 h)	2.5
5	0.25 µmol·L^{-1} ATRA + 100 ng·mL^{-1} LPS (1.5 h)	2.5
6	0.25 µmol·L^{-1} ATRA + 100 ng·mL^{-1} LPS (3 h)	2.5
7	Blank – RIPA buffer	10
8	Blank – RIPA buffer	10
9	BCA working reagent	10
10	BCA working reagent	10

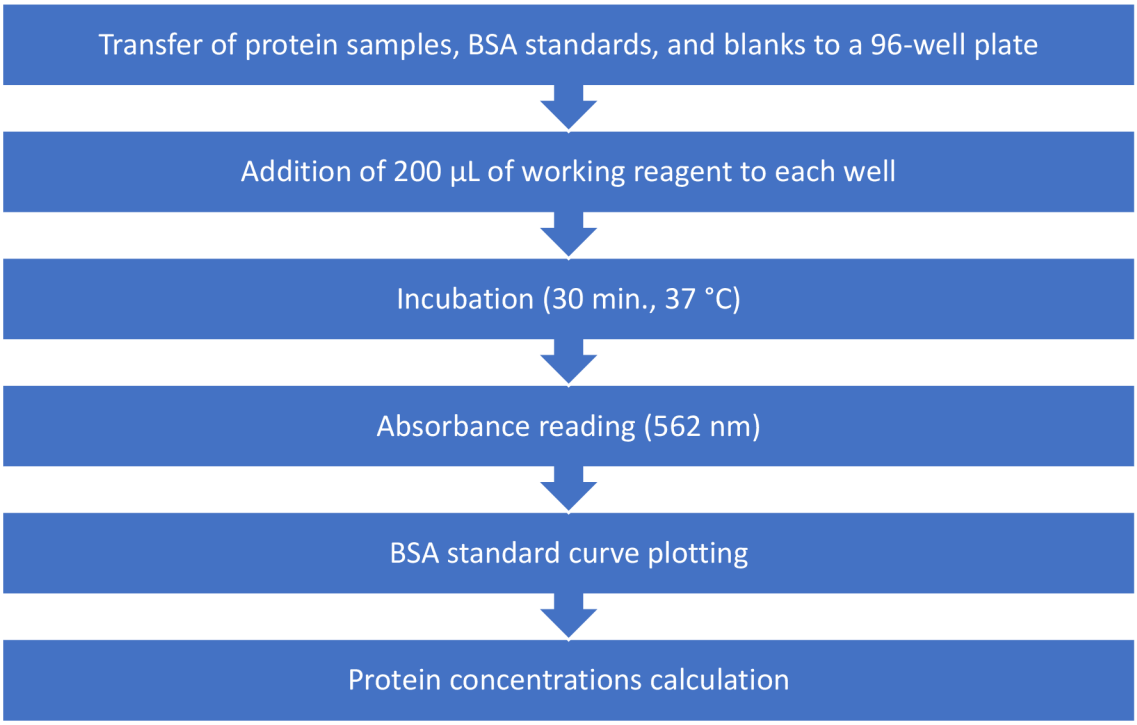

Figure 18. Scheme of the protein quantification workflow.

3.8 SDS-PAGE gel electrophoresis

Separating gel components (for 15 mL: 5.7 mL of distilled water, 5.1 mL of 30% acrylamide – AA, 3.9 mL of 1.5 mol·L^{-1} Tris – pH 8.8, 150 µL of 10% ammonium persulphate – APS, 150 µL of 10% SDS, 15 µL of *N, N, N′, N′*-tetramethylethane-1,2-diamine – TEMED) were mixed in a beaker and transferred between a Spacer and short glass plates to form a gel cassette (Mini-PROTEAN® Tetra System; Bio-Rad; Hercules, CA, USA). Isopropanol was layered on top to protect the separating gel from drying and to avoid air bubbles formation. The isopropanol was subsequently poured out of the cassette followed by gel polymerisation. Stacking gel components (for 5 mL: 2.975 mL of distilled water, 670 µL of 30% AA, 1.25 mL of 0.5 mol·L^{-1} Tris – pH 6.8, 50 µL of 10% APS, 50 µL of 10% SDS, 5 µL of TEMED) were mixed in a beaker and transferred onto the top of the cassette onto the separating gel layer. After that, the comb was inserted immediately. The stacking gel was allowed to polymerise (15 min.).

HL-60 homogenate samples (see Tab. 1) were mixed with 5 µL of a loading dye (5X loading dye: 100 mmol·L^{-1} dithiothreitol – DTT– in a ratio 1:10, 0.1% bromophenol blue, 40% glycerol, 8% SDS, 250 mmol·L^{-1} Tris-Cl – pH 6.8). The samples (and the loading dye) were heated at 75 °C for 10 min. using a Dry Block Thermostat Bio TDB-100 (Biosan; Riga, Latvia). The samples were allowed to cool down at RT for 2 min. After that, the samples were centrifuged (~ 19,318 × g, 5 min., RT). Meanwhile, the comb was removed from the electrophoretic cassette (in a frame) that was placed into a tank with running buffer (for 1 L: 25 mmol·L^{-1} Tris base, 170 mmol·L^{-1} glycine, 0.1% SDS). The samples (protein supernatants; 20 µL), and the ladder PageRuler™ Plus Prestained Protein Ladder (3 µL; No. 26619; Thermo Fisher Scientific; Waltham, MA, USA) were loaded to the polyacrylamide gel (Fig. 19–20). Dye (20 µL) was loaded onto empty lanes.

The electrophoretic system was connected to a power supply (PowerPac™ Universal; Bio-Rad; Hercules, CA, USA) using the following setup: electric current (100 mA), voltage (100 V), and electric power (10 W).

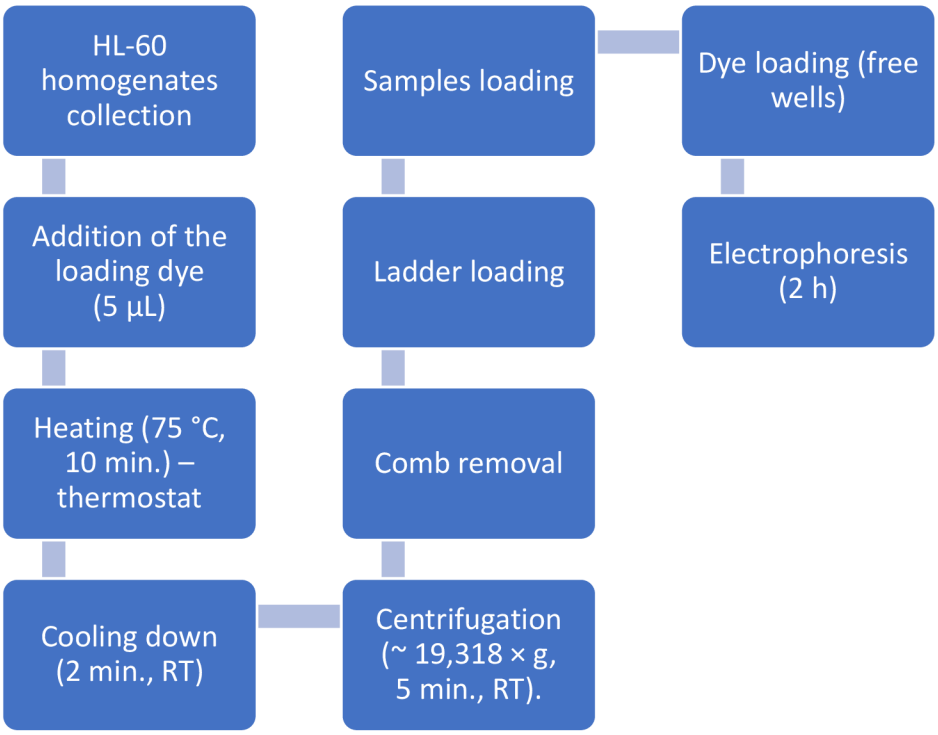

Figure 19. Scheme of the electrophoresis samples preparation workflow.

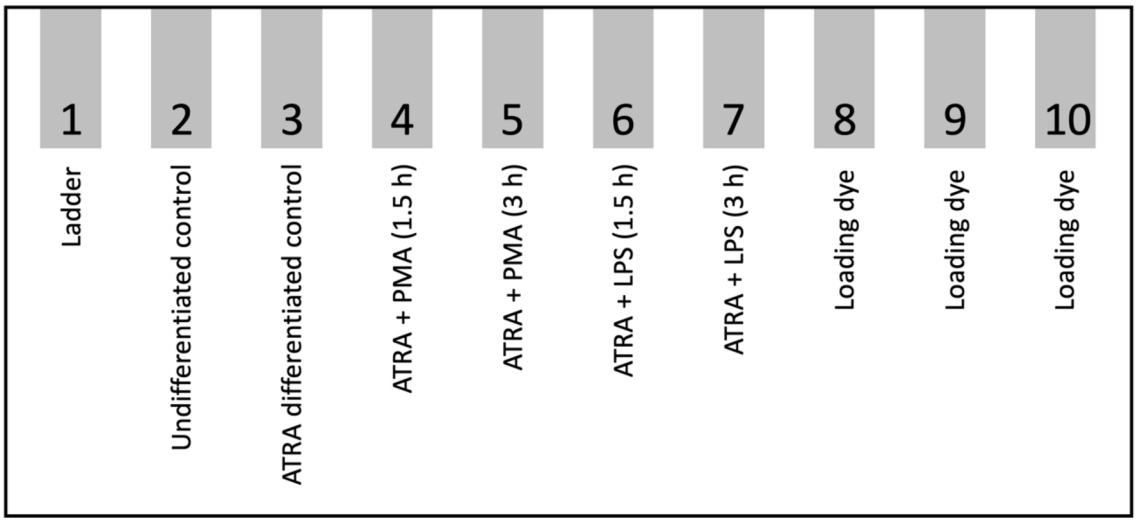

Figure 20. Scheme of the electrophoretic sample loading order.

3.9 Detection of free radical modified protein adducts by western blotting

Proteins separated on the polyacrylamide gel (see 3.8. SDS-PAGE gel electrophoresis) were transferred onto a nitrocellulose membrane by a Trans-Blot® Turbo™ Transfer System (Bio-Rad; Hercules, CA, USA) using the following setup: electric current (1.3 A), voltage (25 V), time (10 min.).

After 10 min., the membrane was removed from the western blotting transfer system (Fig. 21) and rinsed with distilled water on a rocker for 5 min, RT. Consequently, the membrane was stained with Ponceau S stain (0.5% (*w/v*) Ponceau S dissolved in 1% (*v/v*) acetic acid) on the rocker for 5 min, RT. After washing with distilled water (orbital shaker, 5 min., RT), the membrane was scanned using an Amersham Imager 600 (GE Healthcare; UK) with a CCD camera for the confirmation of the protein transfer (using colorimetric imaging with an autoexposure). After the imaging, the membrane was blocked in 20 mL of blocking solution (for 200 mL: 10 g of BSA, 200 mL of 1X Tris buffer saline + Tween-20 – TBST) on the orbital shaker for 2 h at RT. 1X TBST composition (for 500 mL): 50 mL of 10X TBST, 450 mL of distilled water, 0.5 mL of Tween-20. Post blocking, the membrane was incubated with a primary anti-malondialdehyde (MDA) antibody (rabbit anti-MDA IgG; dilution 1:5,000 – 10 µL of Ab, 50 mL of 5% BSA in 1X TBST) overnight at 4 °C (in a fridge). Post incubation, the membrane was left on RT for 20 min. The primary antibody was collected and the membrane was washed with 1X TBST buffer twice (on the orbital shaker, 10 min., RT). After that, the membrane was incubated with the secondary goat anti-rabbit IgG (H+L)-HRP (horseradish peroxidase) conjugate (dilution 1:10,000 – 2 µL of Ab, 20 mL of 5% BSA in 1X TBST) on the orbital shaker for 1 h at RT. Consequently, the membrane was washed with 1X TBST three times (orbital shaker, 10 min., RT).

The formed complexes were developed using Immobilon® Western Chemiluminescent HRP Substrate. The complexes were documented using the Amersham Imager 600 with a CCD camera – chemiluminescent imaging with the autoexposure and the incremental exposure.

The membrane images were further processed in ImageJ software and densitograms were created (Fig. 22).

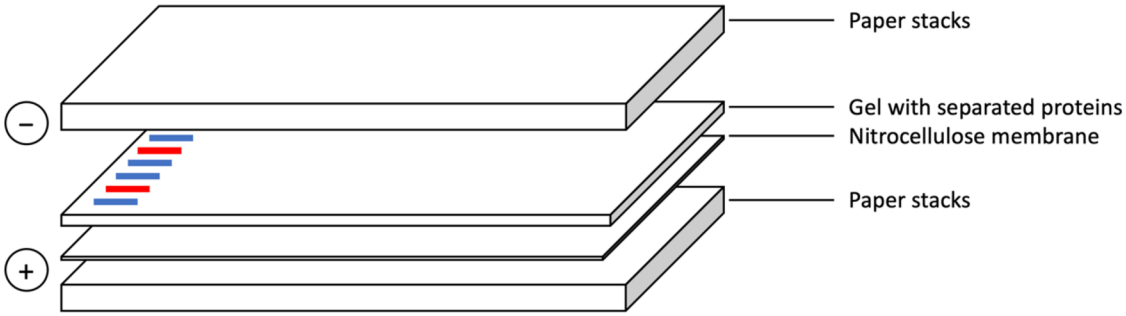

Figure 21. Scheme of the western blotting transfer system.

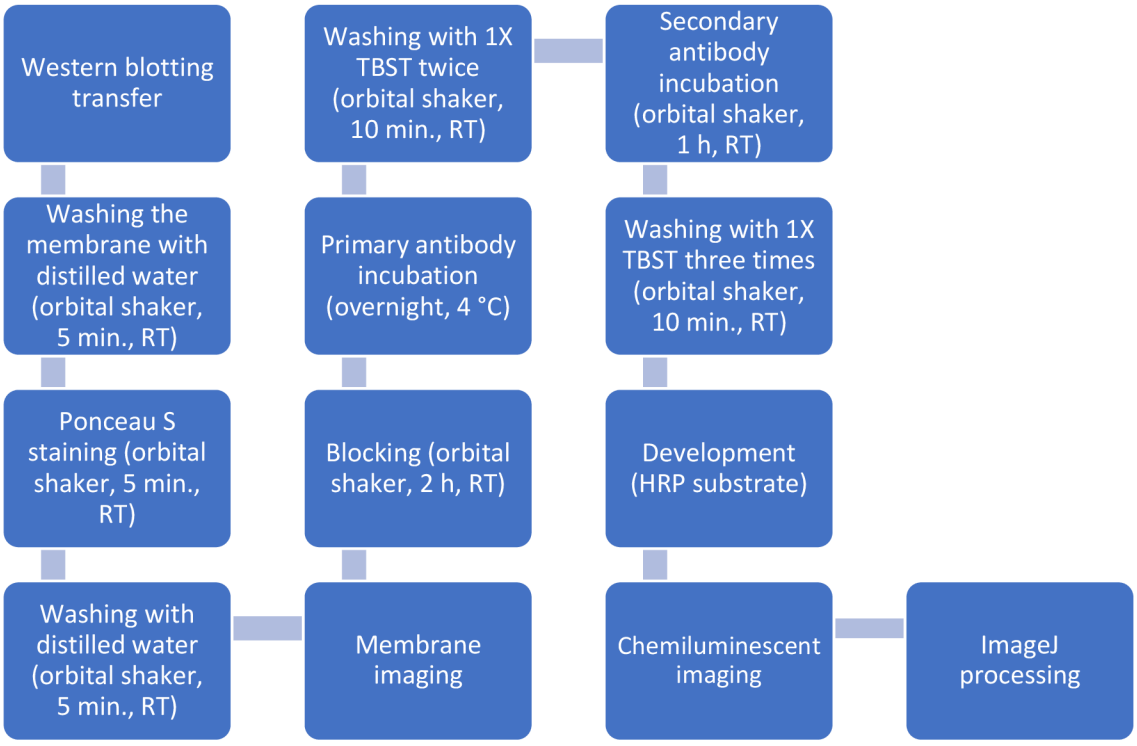

Figure 22. Scheme of the immunodetection workflow.

4 RESULTS

4.1 Cell viability assay

Cell viability and cytotoxicity were detected by the MTT Assay. The assay measures the metabolic activity of cells as an indicator of cell proliferation, viability, and cytotoxicity. Viable cells can reduce tetrazolium dye, MTT, to formazan. Solubilization of formazan crystals, resulting in a coloured solution, is quantified by measuring absorbances at 590 nm. The absorbance values refer to the enzyme metabolic activity of living cells. As mentioned above, HL-60 cells were incubated with PMA (500–18.75 $nmol \cdot L^{-1}$), LPS (1,000–37.5 $ng \cdot mL^{-1}$) for 24 h and ATRA (3–0.09 $\mu mol \cdot L^{-1}$) for 72 h. Based on the MTT and CLSM measurements, a concentration of 50 $nmol \cdot L^{-1}$ PMA (Fig. 23A), 0.25 $\mu mol \cdot L^{-1}$ of ATRA (Fig. 23B) and 100 $ng \cdot mL^{-1}$ of LPS (Fig. 23C) was chosen for further experiments. Concentration-dependent cytotoxic effects were observed among treatment conditions. At higher concentrations, a significant loss of viability (~ 40%) was observed in all experimental conditions.

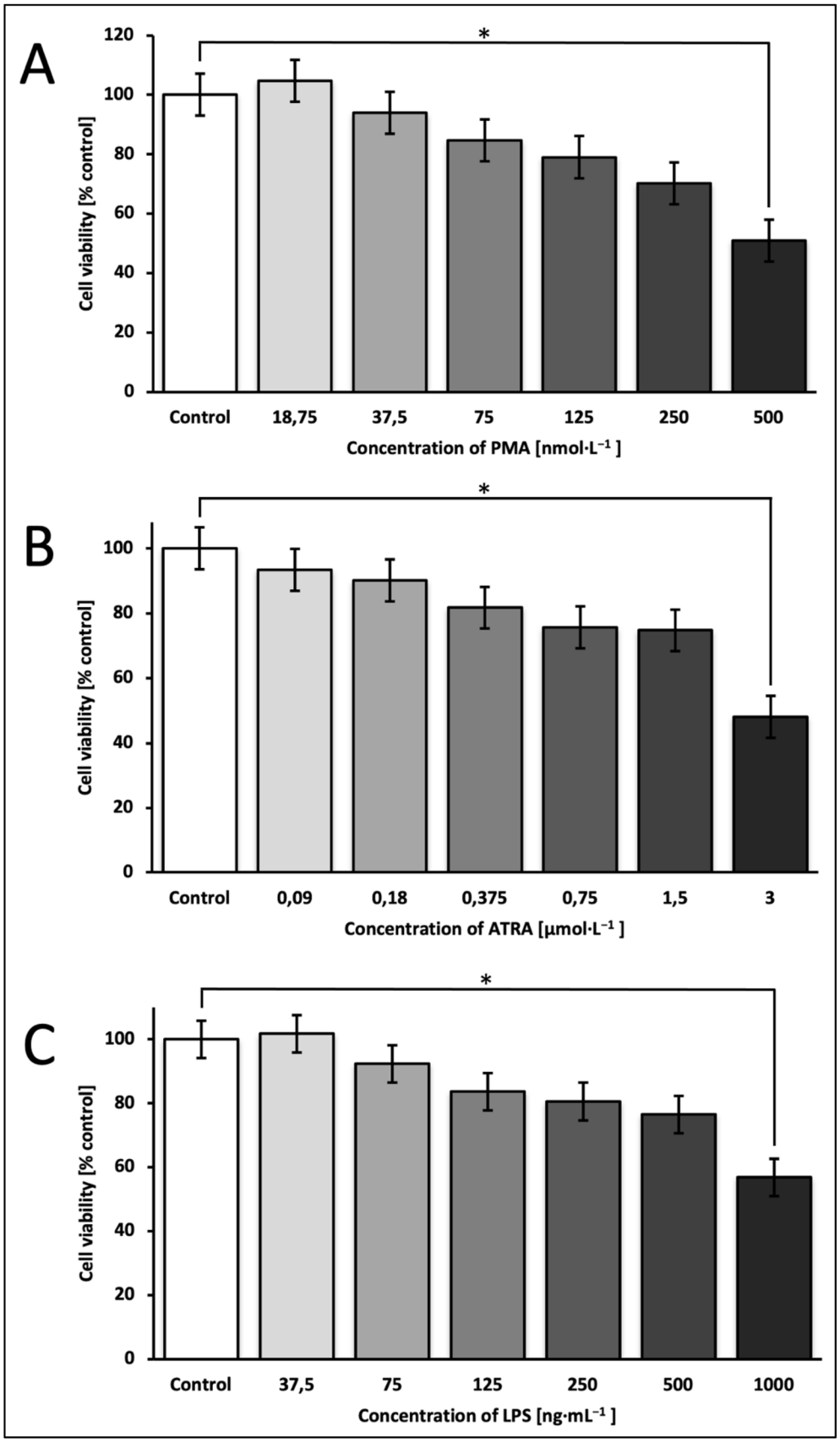

Figure 23. Cell viabilities of HL-60 cells (percentages relative to control undifferentiated HL-60 cells) after the treatment with: **(A)** PMA (500–18.75 nmol·L^{-1}), **(B)** ATRA (3–0.09 µmol·L^{-1}), **(C)** LPS (1,000–37.5 ng·mL^{-1}). (n = 2). The data are represented as mean ± standard error (SE). *p = 0.05*.

4.2 Cell culture and differentiation

To differentiate HL-60 cells into neutrophils, the cells were treated with 0.25 $\mu mol \cdot L^{-1}$ ATRA in the complete RPMI medium for 72 h. CLSM analysis (Nomarski DIC observations) revealed changes in the cell morphology of the differentiated HL-60 cells in comparison with the untreated cells (Fig. 24A–B).

Differentiated neutrophils were stimulated with PMA (50 $nmol \cdot L^{-1}$) or LPS (100 $ng \cdot mL^{-1}$) for 3 h at 37 °C and 5% CO_2. Throughout this process, samples were collected at intervals of 1.5 and 3 h. Unstimulated cells and cells differentiated with ATRA were used as controls. The microscopic observations showed differences in cell morphology between control and differentiated cells (Fig. 24C–D).

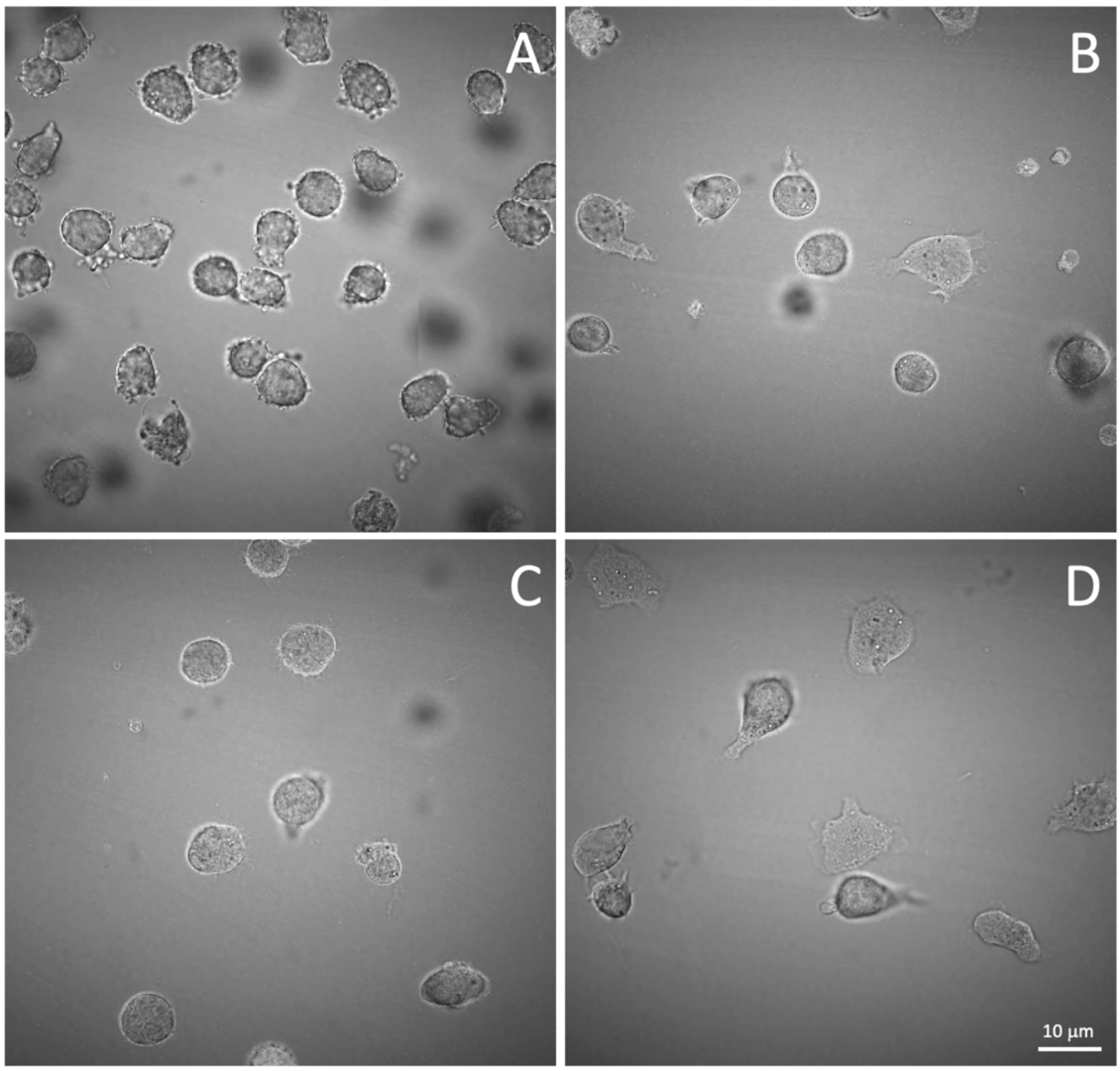

Figure 24. Differentiation of HL-60 cells into neutrophils and subsequent neutrophil activation. **(A)** Undifferentiated control. **(B)** ATRA differentiated control. **(C)** ATRA + PMA (3 h). **(D)** ATRA + LPS (3 h). Visualization by Nomarski DIC microscopy. Scale bar: 10 µm (for all images).

4.3 Superoxide anion radical detection using electron paramagnetic resonance spin trapping spectroscopy

The formation of superoxide anion radical during HL-60 cells differentiation into neutrophils and subsequent neutrophil stimulation was monitored using EPR spectroscopy. Generated $O_2^{\bullet -}$ interacts with EMPO forming EMPO-OOH adducts. No signal was observed in control HL-60 cells. Differentiation of HL-60 into neutrophils with ATRA resulted in the appearance of the EMPO-OOH spectra (Fig. 25). Four peaks with hyperfine splitting corresponds to the EMPO-OOH adducts. Upon stimulation, a moderately strong signal was detected with PMA-induced cells (Fig. 25). The strongest signal was recorded in the case of LPS-activated cells (Fig. 25). The signal in undifferentiated HL-60 cells was negligible (Fig. 25). In the case of ATRA differentiated control HL-60 cells, the EMPO-OOH adduct EPR signal ranged from − 1,200 to + 1,690 (Fig. 26A). The EMPO-OOH adduct EPR signal range was between – 3,347 and + 4,085 with the PMA-induced HL-60 cells (Fig. 26B). In the case of LPS-activated HL-60 cells, the EMPO-OOH adduct EPR signal ranged from − 9,287 to + 10,234 (Fig. 26C). The effect of different activation stimuli (PMA and LPS) on the EMPO-OOH adduct EPR signal level was noticeable. In the case of LPS, the intensity of the EMPO-OOH adduct was more than twice as high as in the case of PMA, indicating higher $O_2^{\bullet -}$ production (Fig. 25).

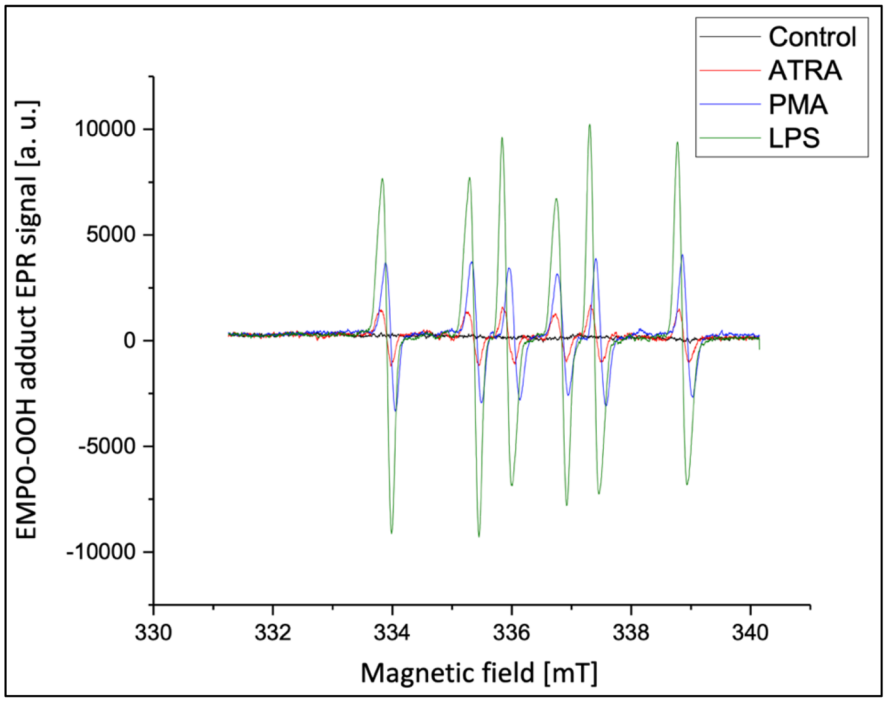

Figure 25. EMPO-OOH adduct detection in: undifferentiated control **(black trace)**, ATRA differentiated control **(red trace)**, ATRA + PMA **(blue trace)** and ATRA + LPS **(green trace)** using EPR spin trapping.

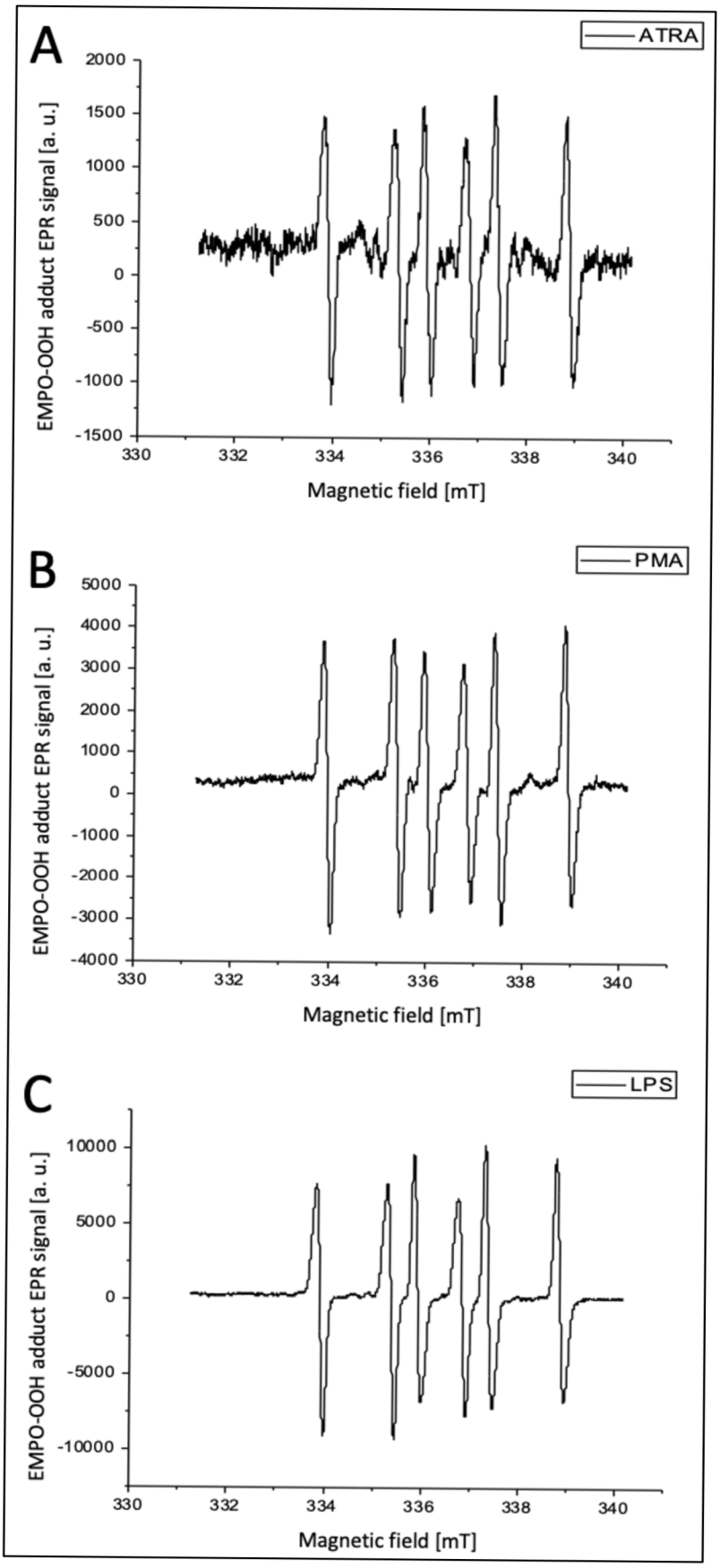

Figure 26. EMPO-OOH adduct detection using EPR spin trapping. **(A)** ATRA differentiated control. **(B)** ATRA + PMA. **(C)** ATRA + LPS.

4.4 Confocal laser scanning microscopy

Cell membrane integrity and nuclear changes of differentiated and stimulated HL-60 cells were observed by CLSM using fluorescent dyes FM4-64 and Hoechst 33342, respectively. All the samples were observed in three channels: Nomarski DIC (Fig. 27, 29), Hoechst 33342 – blue (Fig. 27, 29), and FM4-64 – red (Fig. 27, 29). Subsequently, merged images of the Hoechst 33342 and FM4-64 channels were taken (Fig. 27, 29). Finally, merged images of all three channels: Nomarski DIC, Hoechst 33342, and FM4-64 were taken (Fig. 28, 30).

HL-60 undifferentiated control was observed under a lower (Fig. 27A) and a higher (Fig. 27B) microscope magnification using all three channels mentioned above. The cells retained their typical spherical shape as well as their membrane integrity. Nuclei and membrane localizations were observed during the merging of all three channels together (Fig. 28).

HL-60 control differentiated with 0.25 $\mu mol \cdot L^{-1}$ ATRA and HL-60 cells subsequently activated with 50 $nmol \cdot L^{-1}$ PMA or 100 $ng \cdot mL^{-1}$ LPS (Fig. 29, 30) were also documented using all three channels mentioned above. In the case of the differentiated control (Fig. 29, 30A), the shape of the cells was typically spherical, but oval cells were also observed. Cell extension was observed in some cells. During observation of the PMA-activated cells (Fig. 29, 30B), it appeared that the shape of the cells was also typically spherical, but cell extensions were already more visible and more frequent than in the differentiated control. During observation of LPS-activated cells (Fig. 29, 30C), a change in the cell shape from spherical to oval was evident. Pseudopodia were also formed (Fig. 29, 30C). In this case, single granules were visible (Fig. 29, 30C).

Cell differentiation and activation were associated with changes in cell morphology. However, cell integrity was maintained using our chosen concentrations of differentiation and activation agents (Fig. 27–30).

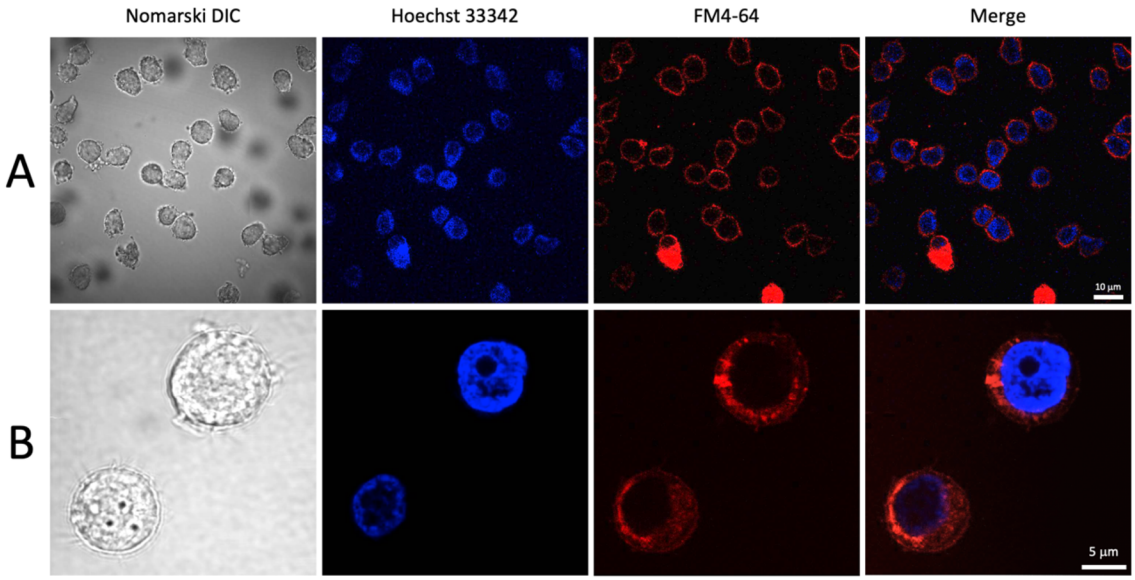

Figure 27. Confocal laser scanning microscopy images of HL-60 undifferentiated control cells. **(A)** Lower microscope magnification. **(B)** Higher microscope magnification. Imaging using Nomarski DIC, fluorescent labelling Hoechst 33342 and FM4-64 (5 min., RT) for nuclear changes and membrane integrity observations, respectively. Scale bar: **(A)** 10 µm (for all images), **(B)** 5 µm (for all images).

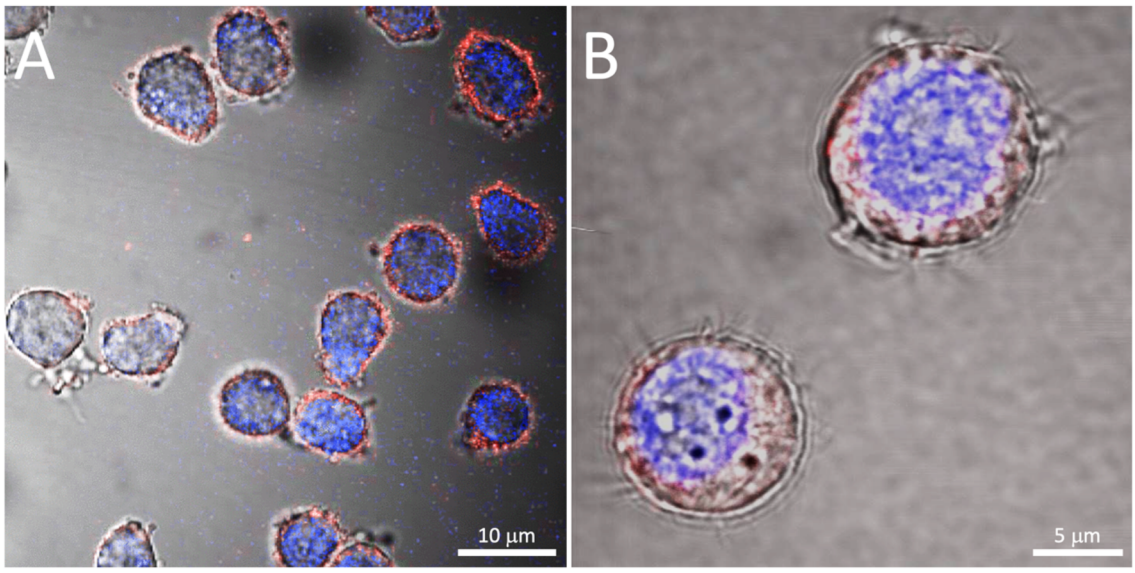

Figure 28. Confocal laser scanning microscopy images of HL-60 undifferentiated control cells (merged images of Nomarski DIC, Hoechst 33342, and FM4-64 channels). **(A)** Lower microscope magnification. **(B)** Higher microscope magnification. Imaging using Nomarski DIC, fluorescent labelling Hoechst 33342 and FM4-64 (5 min., RT) for nuclear changes and membrane integrity observations, respectively. Scale bar: **(A)** 10 µm, **(B)** 5 µm.

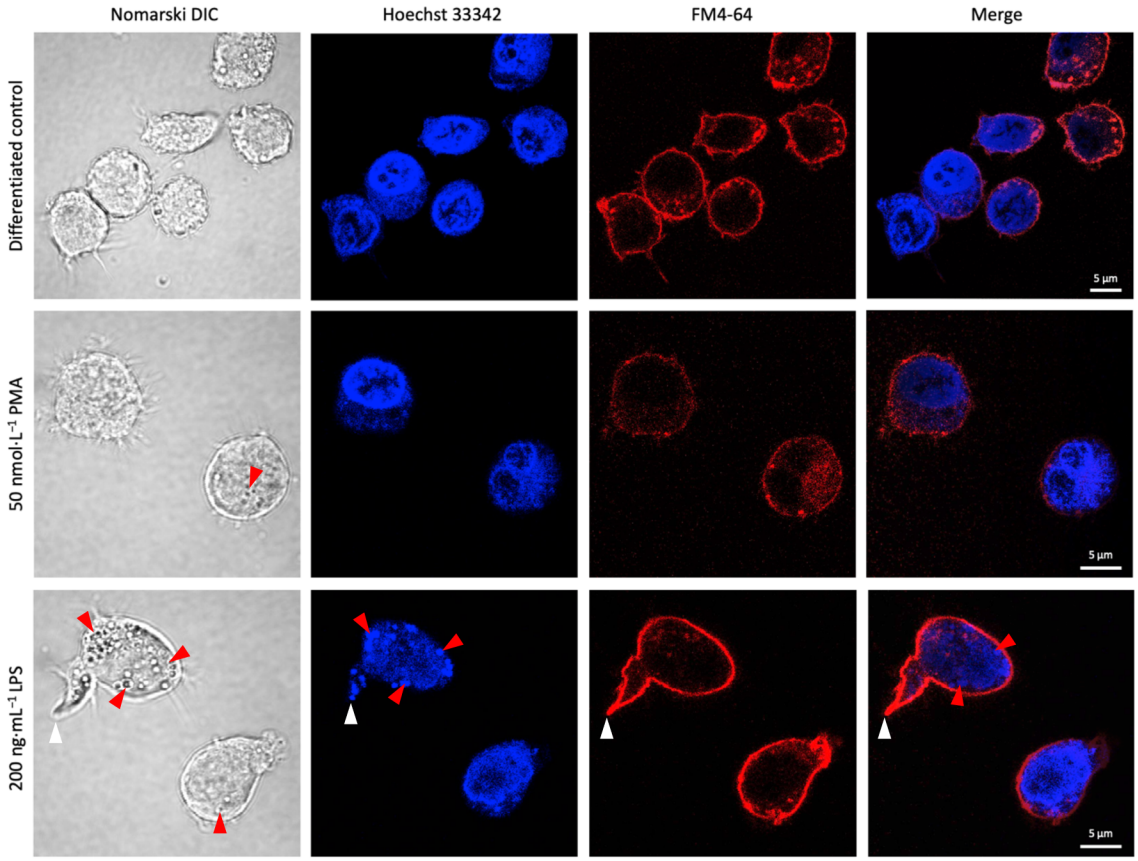

Figure 29. Confocal laser scanning microscopy images of HL-60 cells differentiated with 0.25 µmol·L^{-1} ATRA and subsequently activated with 50 nmol·L^{-1} PMA or 100 ng·mL^{-1} LPS. Imaging using Nomarski DIC, fluorescent labelling Hoechst 33342 and FM4-64 (5 min., RT) for nuclear changes and membrane integrity observations, respectively. Scale bar: 5 µm (for all images). White arrows indicate pseudopodia. Red arrows indicate neutrophil granules.

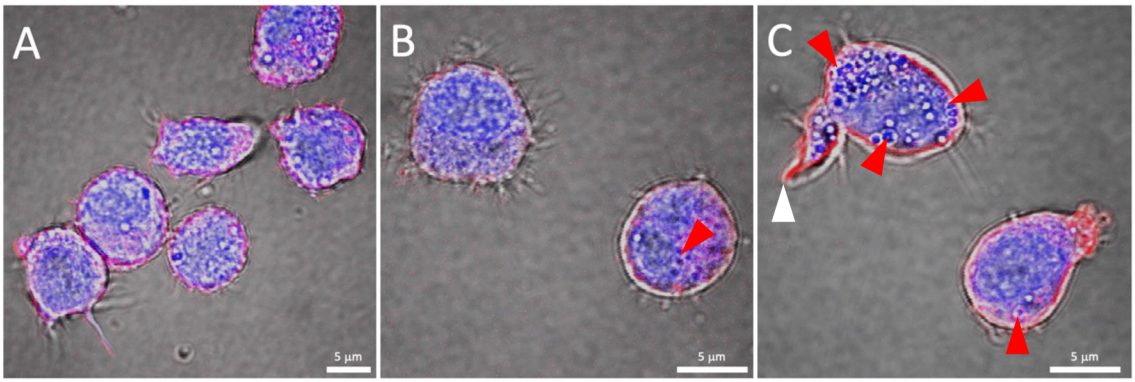

Figure 30. Confocal laser scanning microscopy images of HL-60 cells differentiated with 0.25 µmol·L^{-1} ATRA and subsequently activated with 50 nmol·L^{-1} PMA or 100 ng·mL^{-1} LPS (merged images of Nomarski DIC, Hoechst 33342, and FM4-64 channels). Imaging using Nomarski DIC, fluorescent labelling Hoechst 33342 and FM4-64 (5 min., RT) for nuclear changes and membrane integrity observations, respectively. **(A)** ATRA differentiated control. **(B)** ATRA + PMA. **(C)** ATRA + LPS. Scale bar: 5 µm (for all images). White arrow indicates the pseudopodium. Red arrows indicate neutrophil granules.

4.5 Protein quantification

Prior to electrophoresis, protein concentration in control and differentiated samples was determined by Pierce™ BCA Protein Assay Kit. The copper ions (reduction of Cu^{2+} ions to $Cu^{1+)}$ react with bicinchoninic acid (BCA), resulting in a purple colour change of the solution. The copper ions react mainly with four amino acid residues (cysteine, cystine, tyrosine and tryptophan) and also with peptide bonds of proteins. The concentrations of unknown samples are determined by comparing the absorbances of these samples with the absorbances of standards of known concentrations (BSA in our case). The absorbance is detected at a wavelength of 562 nm since at this wavelength the BCA complex has its maximal absorbance (He, 2011). The protein concentrations in differentiated and subsequently activated HL-60 cells ranged from 758 $\mu g \cdot mL^{-1}$ to 563 $\mu g \cdot mL^{-1}$.

4.6 Detection of free radical modified protein adducts by western blotting

Based on protein quantification data, a defined concentration of proteins (20 µg) was loaded onto 10% SDS-PAGE gels to prevent loading variability among samples. Proteins present in the whole cell lysate got separated based on their molecular weight and were subjected to western blotting analysis. Free radical modified protein adduct formation was detected using an anti-MDA primary rabbit IgG antibody. Malondialdehyde is a byproduct of lipid peroxidation. It modifies proteins resulting in protein adducts formation. The primary antibody used in this study binds to MDA and aids in the visualization of MDA adducts formation along the differentiation process. Protein transfer from gel to membrane was confirmed by Ponceau S staining (Fig. 31).

Two groups of proteins (around 35 kDa and 12 kDa) were selected because their band intensities differed among the activated HL-60 cells, undifferentiated and ATRA differentiated controls (Fig. 32). Subsequently, densitograms were created to graphically illustrate the differences in protein band intensities between 35 kDa and 12 kDa proteins (Fig. 33). Densitogram sections showing these selected protein groups were compared among all the samples (Fig. 34–35). These data revealed that protein band intensity of the 35 kDa region was low in the undifferentiated control (Fig. 34A), whereas the peak was

already more noticeable in the differentiated control (Fig. 34B), and this trend of stronger intensity continued due to activation of HL-60 differentiated neutrophils (Fig. 34C–F).

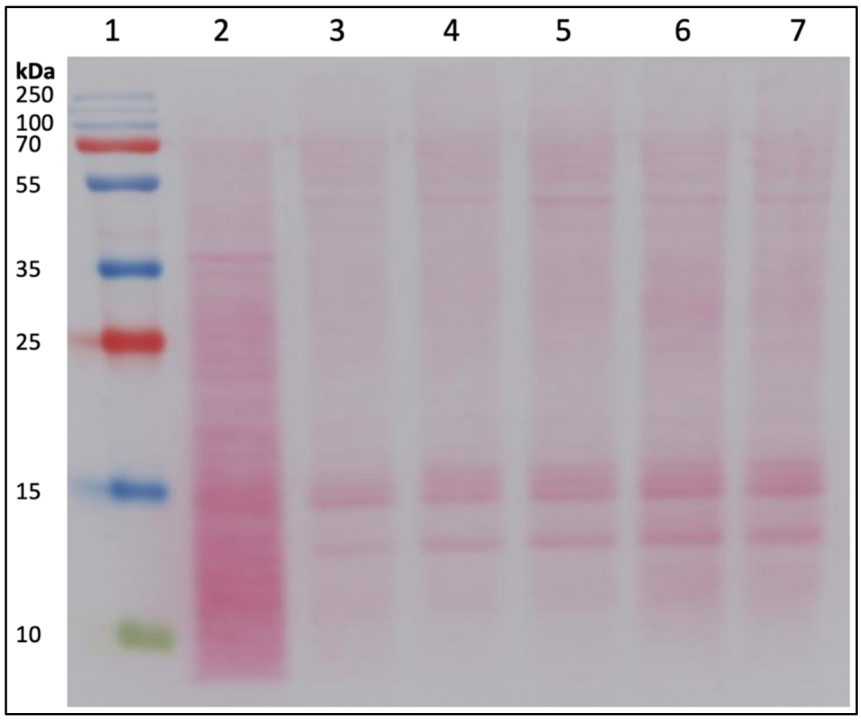

Figure 31. Ponceau S staining (for the confirmation of the protein transfer). **(1)** Protein ladder. **(2)** Undifferentiated control. **(3)** ATRA differentiated control. **(4)** ATRA + PMA (1.5 h). **(5)** ATRA + PMA (3 h). **(6)** ATRA + LPS (1.5 h). **(7)** ATRA + LPS (3 h).

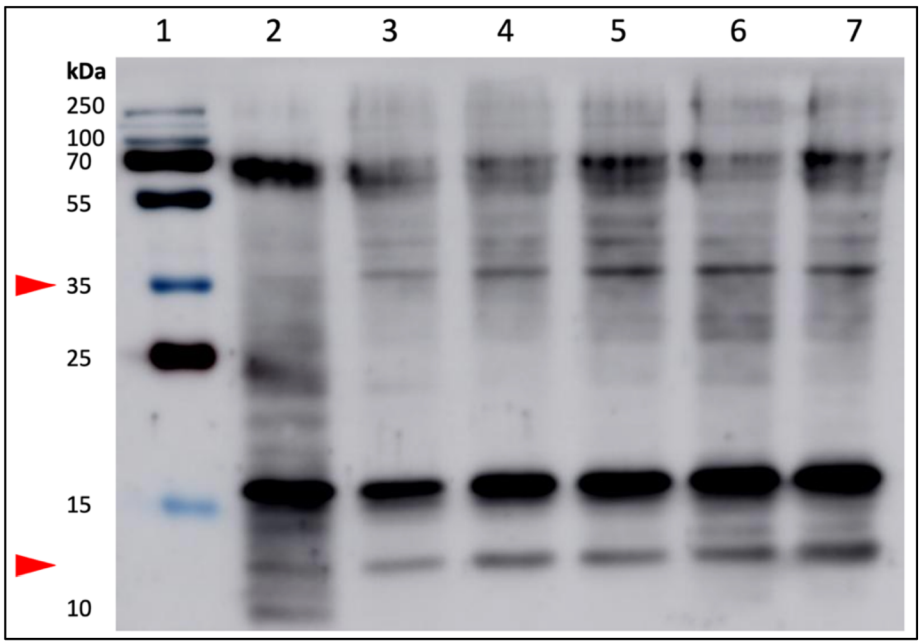

Figure 32. Detection of the free radical modified protein adducts using western blotting. **(1)** Protein ladder. **(2)** Undifferentiated control. **(3)** ATRA differentiated control. **(4)** ATRA + PMA (1.5 h). **(5)** ATRA + PMA (3 h). **(6)** ATRA + LPS (1.5 h). **(7)** ATRA + LPS (3 h). Red arrows indicate two protein groups that were selected because of the differences in band intensities.

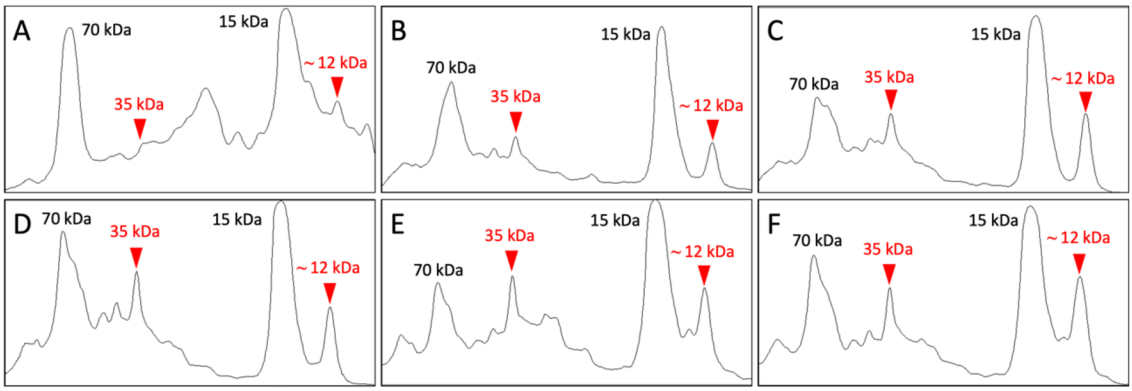

Figure 33. Densitograms of the free radical modified protein adducts. **(A)** Undifferentiated control. **(B)** ATRA differentiated control. **(C)** ATRA + PMA (1.5 h). **(D)** ATRA + PMA (3 h). **(E)** ATRA + LPS (1.5 h). **(F)** ATRA + LPS (3 h). Red arrows indicate two protein bands that were selected because of the differences in intensities. Densitograms were created using ImageJ (Abramoff *et al.*, 2004).

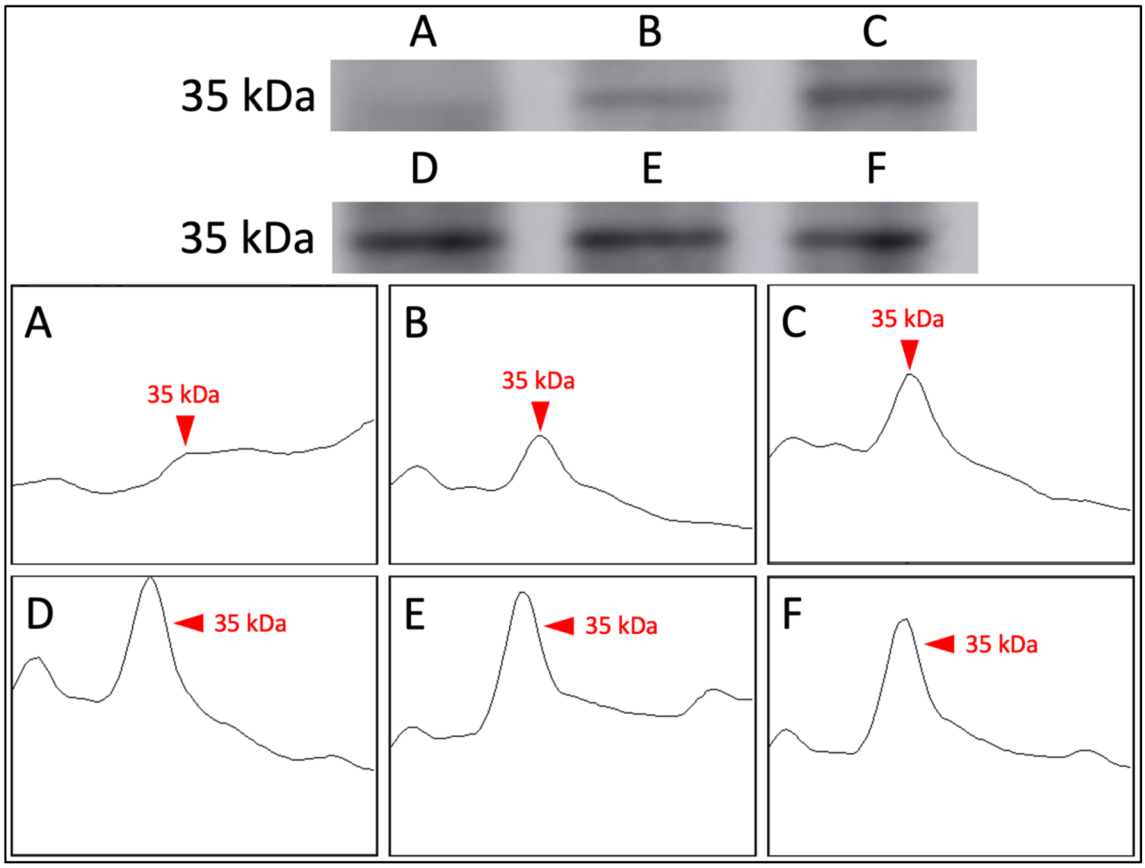

Figure 34. Bands **(top)** and densitograms **(down)** of the 35 kDa free radical modified protein adducts. **(A)** Undifferentiated control. **(B)** ATRA differentiated control. **(C)** ATRA + PMA (1.5 h). **(D)** ATRA + PMA (3 h). **(E)** ATRA + LPS (1.5 h). **(F)** ATRA + LPS (3 h).

A similar pattern of difference in band intensity was observed with the 12 kDa proteins. This time the band intensity was stronger in the undifferentiated control (Fig. 35A) than in the differentiated control (Fig. 35B). In PMA-activated HL-60 cells for 1.5 h and 3 h (Fig. 35C and 35D) or LPS-activated HL-60 cells for 1.5 h (Fig. 35E), the intensity was approximately comparable to the control, whereas, in the case of LPS-activation for 3 h (Fig. 35F), the band intensity was the strongest, documenting the effect of the activation time on the protein composition.

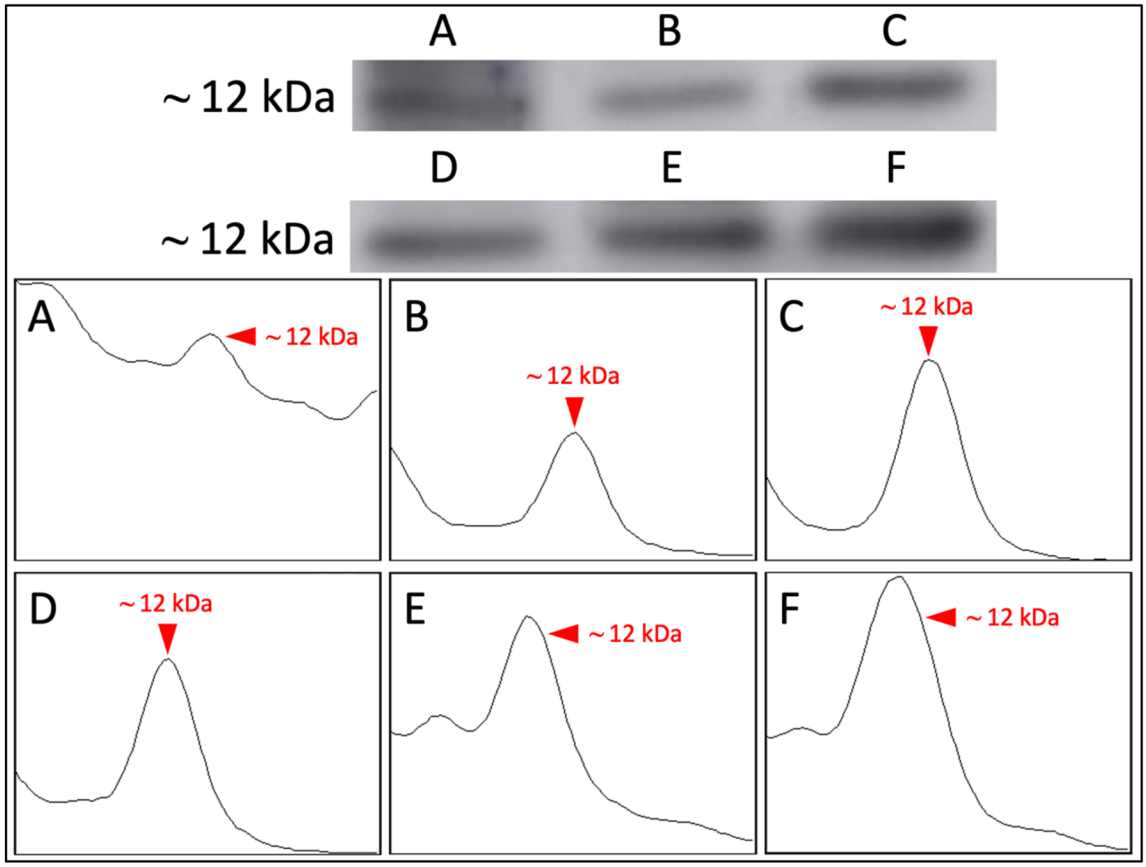

Figure 35. Bands **(top)** and densitograms **(down)** of the 12 kDa free radical modified protein adducts. **(A)** Undifferentiated control. **(B)** ATRA differentiated control. **(C)** ATRA + PMA (1.5 h). **(D)** ATRA + PMA (3 h). **(E)** ATRA + LPS (1.5 h). **(F)** ATRA + LPS (3 h).

5 DISCUSSION

The methods used to differentiate the HL-60 cell line into neutrophils using ATRA and subsequent stimulation of neutrophils with PMA or LPS were proven to be sufficiently effective. The viability of HL-60 cells under experimental conditions was confirmed by the MTT assay. The functionality of the ATRA-based differentiation protocol and PMA- and LPS-based activation protocols is well-known and validated, which can be illustrated by the large number of studies that have employed these methods. It is important to consider the possible side effects that each substance may induce. Some studies suggest that a general feature of ATRA observed in other cell types may be the disruption of the cell membrane by increasing its permeability (Prat *et al.*, 2015). Utilization of higher concentrations of ATRA, PMA and LPS was reported to enhance ROS and cytokine production, subsequently leading to the cell death by oxidative stress (Almzaiel *et al.*, 2013; Mroczek *et al.*, 2020; Ruiz-Alcaraz *et al.*, 2022).

Considering these facts, morphological assessment of cells was carried out using confocal microscopy. CLSM observations were particularly useful in terms of investigating the integrity of cell membranes (using FM4-64). These observations confirmed the maintenance of cell membrane integrity and the absence of membrane disruption due to permeability. This phenomenon confirms the fact that our selected concentrations of ATRA for differentiation and PMA with LPS for stimulation did not induce an excessive cytotoxic effect on the cells.

As demonstrated by several studies, neutrophil PMA-activation leads to suicidal NETosis, whereas LPS-stimulation results in the induction of vital NETosis. These processes are distinguished from each other at the molecular level. PMA application causes oxidative stress damaging cellular material, resulting in the suicidal NETosis. The addition of LPS triggers neutrophils to produce cytokines. Although the superoxide anion radical production is increased in the case of LPS-stimulation compared to PMA-activation, NETosis remains vital, which is caused by the Toll-like receptor 4 (TLR-4) activation mechanism. This mechanism activates signalling pathways associated with cell survival. Pseudopodia formation is typical for LPS-stimulated neutrophils, as can be observed in the studies of Wang *et al.* (2017) and Arroyo *et al.* (2019). A similar phenomenon was also observed in our present study. Neutrophils form pseudopodia to modify their cell shape during phagocytosis (Dewitt & Hallett, 2020). Although the formation of pseudopodia is also characteristic of PMA-induced neutrophils – PMA

activates protein kinase C (PKC), which leads to actin polymerization and the formation of pseudopodia – several studies suggest that their presence is not as frequent as in the case of LPS-stimulation (Damascena *et al.*, 2022). This finding is supported by our results, as pseudopodia were observed only upon neutrophil LPS-activation.

We have optimized the neutrophil activation time (max. 3 h) based on data from recent studies wherein the NETosis activity was reported to be active within 4 h and then the activity decreases (Delgado-Rizo *et al.*, 2017). To gain more insight into the differentiation of HL-60 cells into neutrophils, analysis of neutrophil markers could be performed, e.g. by flow cytometry, or RT-PCR analysis using other activating and differentiating agents.

Differences in the size of natural human neutrophils and neutrophils differentiated from HL-60 cells described in the literature were also noticed in our case. Natural neutrophils in suspensions tend to be smaller, around 9 μm in diameter (Niemiec *et al.*, 2015), whereas neutrophils differentiated from HL-60 cells can reach up to 10–12 μm in diameter (Babatunde *et al.*, 2021), which was confirmed by our microscopic observations. Other differences include, e.g. lower expression of surface markers (Rincón *et al.*, 2018), and they vary among differentiation protocols.

EPR measurements using the spin trap EMPO confirmed superoxide anion radical generation along HL-60 differentiation into neutrophils and its consequent activation. The differences in EPR signal intensity between LPS-stimulated neutrophils and PMA-stimulated neutrophils were remarkable. This difference can be explained, e.g. by the different mechanism of NADPH oxidase activation. LPS-stimulation of neutrophils leads to activation via TLR-4, which causes an abundance of superoxide anion radicals (Nadeem *et al.*, 2017) compared to PMA-stimulation of neutrophils, upon which NADPH oxidase is activated by PKC (Gray *et al.*, 2013).

The character of both types of NETosis (PMA-induced suicidal vs. LPS-induced vital) indicates the occurrence of neutrophil granules in the cells. While PMA-stimulation leads to a decrease in the number of granules in neutrophils due to ROS production, LPS-stimulation, on the other hand, promotes granule accumulation through increased cytokine production, as can be noticed in the CLSM images of Azzouz *et al.* (2021). These differences can be monitored both morphologically and biochemically. This assumption was supported by our results, both by CLSM microscopic observations of stimulated neutrophils and by SDS-PAGE and western blot analysis of MDA-protein adducts.

In the proteomic analysis section of our study, it was found that groups of MDA-protein adducts around 35 kDa and 12 kDa were present in activated neutrophils. Band intensities of these proteins in the western blot detection differed remarkably from those of controls. Free radical-modified protein adducts with notable differences in band intensities identified in our present study should be subjected to mass spectrometric analysis to identify specific protein targets undergoing lipid peroxidation events. Literature-based analysis reveals that azurocidin protein (also known as CAP37) is detected in the region around 37 kDa in activated neutrophils (Nalmpantis *et al.*, 2020). Its presence would be indicated by the occurrence of azurophilic granules, possibly also secretory vesicles (Ma *et al.*, 2013), in the neutrophils obtained by us. The release of azurocidin by neutrophils is a defence mechanism against microbial infections. Azurocidin exhibits direct antimicrobial activity, but also indirect activity related to its involvement in phagocytosis (Zhang *et al.*, 2022). The presence of proteins with molecular weight around 12 kDa could implicate calgranulins (S100A8 calgranulin A, S100A9 calgranulin B and S100A12 calgranulin C), which form calprotectin protein complexes. These proteins are represented in neutrophils in large amounts. The link with lipid peroxidation is two-sided. Some studies portray calgranulins A and B as potent inducers of ROS (Bøyum *et al.*, 2010). However, other studies also mention the ability of calgranulin A to inhibit ROS generation in cell membranes (Perera *et al.*, 2010). The intensity of protein bands in the region around 12 kDa was the highest in the case of LPS-stimulated neutrophils, which corresponds with microscopic observations during which the most granules were seen in LPS-stimulated neutrophils. Calgranulins, as well as azurocidin, are proteins stored in neutrophil granules. It is also necessary to consider the calgranulins role in NETosis. These proteins stimulate the release of nuclear DNA, which subsequently binds to NETs (Sprenkeler *et al.*, 2022).

Concerning the results obtained, it is worth mentioning their potential applications in medical biotechnology. A thorough knowledge of the generation of reactive oxygen species and their role in various diseases may lead to improved therapeutic options. EPR detection (using spin trapping) can be utilized in the evaluation of the effectiveness of drugs targeted to inhibition of ROS generation. Lipid peroxidation and the resulting oxidative stress are associated with neurodegenerative and cardiovascular diseases, but also with cancer. Therefore, molecules with antioxidant activity (including calgranulins) have considerable potential in medical biotechnology. Potentially, the application in disease diagnostics is also possible, as increased levels of these proteins could correlate

with the course of disease-related pathological processes. A final application in medical biotechnology could be a recombinant protein production for therapeutic purposes, which could limit the disease progression associated with oxidative stress. It is worth mentioning a recent study by Charkhizadeh *et al.* (2020) in which the anti-tumour effect of recombinant calprotectin was induced by apoptosis in the leukemia cell line Nalm6. The antimicrobial properties of azurocidin could also be exploited in the field of medical biotechnology. Some studies suggest that azurocidine affects the course of ST segment elevation myocardial infarction (STEMI). Since azurocidin production promotes heart failure, it could become a promising target for the future treatment of STEMI (Ipek *et al.*, 2018).

6 CONCLUSIONS

The main objective of this thesis was to analyse the role of reactive oxygen species during the formation of neutrophil extracellular traps. An overview of the literature on neutrophil extracellular traps, reactive oxygen species and their role in NETosis and lipid peroxidation, the biotechnological potential of NETosis, the HL-60 cell line, and some of the techniques used in the experimental part of our study was carried out in the theoretical part of the study.

The findings from the experimental part of this thesis are summarized below.

1. Using the MTT cell viability assay, the concentrations of the differentiation agent ATRA (0.25 $\mu mol \cdot L^{-1}$) and the activation stimuli PMA (50 $nmol \cdot L^{-1}$) and LPS (100 $ng \cdot mL^{-1}$) were determined to be effective in inducing differentiation of HL-60 cells into neutrophils and neutrophil activation, respectively. Moreover, at these selected concentrations of the aforementioned agents, high cell viability and membrane integrity were maintained.
2. The effect of PMA and LPS on the activation of HL-60 differentiated neutrophils was confirmed to be different. LPS-stimulation leads to the formation of pseudopodia and neutrophil granules during the vital NETosis. These two phenomena occur to a much lesser extent during the PMA-induced suicidal NETosis due to due to the activation mechanism of NADPH oxidase by PKC and associated induction of cell death.
3. The presence of superoxide anion radical in differentiated and subsequently activated neutrophils was monitored using electron paramagnetic resonance spin trapping spectroscopy. The results indicate a strong association between neutrophil stimulation and ROS production. LPS-stimulation resulted in notably higher superoxide anion radical generation than PMA-stimulation, which may be explained by different mechanisms of NADPH oxidase activation (via TLR-4 in the case of LPS and PKC in the case of PMA).
4. Proteomic analysis of the MDA-protein adducts revealed considerable differences in the protein band intensity around 35 kDa and 12 kDa among control HL-60 cells and activated neutrophils using western blotting detection. These bands may contain proteins, such as azurocidin or calgranulins, which, due to their properties, may offer future potential for applications in medical

biotechnology (protection of cells against ROS-mediated oxidation in the case of calgranulins or azurocidin-targeted therapy of heart diseases).

5. Research focusing on identification and charcaterization of the two selected proteins around 35 kDa and 12 kDa and their potential biotechnological applications was proposed.

7 REFERENCES

Abbas, K., Babić, N., & Peyrot, F. (2016). Use of spin traps to detect superoxide production in living cells by electron paramagnetic resonance (EPR) spectroscopy. *Methods*, *109*, 31–43. https://doi.org/10.1016/J.YMETH.2016.05.001

Abramoff, M. D., Magalhães, P. J., & Ram, S. J. (2004). Image processing with ImageJ. *Biophotonics International*, *11*(7), 36–42. https://dspace.library.uu.nl/handle/1874/204900

Almzaiel, A. J., Billington, R., Smerdon, G., & Moody, A. J. (2013). Effects of hyperbaric oxygen treatment on antimicrobial function and apoptosis of differentiated HL-60 (neutrophil-like) cells. *Life Sciences*, *93*(2–3), 125–131. https://doi.org/10.1016/J.LFS.2013.06.003

Arroyo, R., Khan, M. A., Echaide, M., Pérez-Gil, J., & Palaniyar, N. (2019). SP-D attenuates LPS-induced formation of human neutrophil extracellular traps (NETs), protecting pulmonary surfactant inactivation by NETs. *Communications Biology, 2*(1), 1–13. https://doi.org/10.1038/s42003-019-0662-5

Ayala, A., Muñoz, M. F., & Argüelles, S. (2014). Lipid peroxidation: Production, metabolism, and signaling mechanisms of malondialdehyde and 4-hydroxy-2-nonenal. *Oxidative Medicine and Cellular Longevity*. https://doi.org/10.1155/2014/360438

Azzouz, D., Khan, M. A., & Palaniyar, N. (2021). ROS induces NETosis by oxidizing DNA and initiating DNA repair. *Cell Death Discovery, 7*(1), 1–10. https://doi.org/10.1038/s41420-021-00491-3

Babatunde, A. K., Wang, X., Hopke, A., Lannes, N., Mantel, P.-Y., & Irimia, D. (2021). Chemotaxis and swarming in differentiated HL-60 neutrophil-like cells. *Scientific Reports*, *11*, 778. https://doi.org/10.1038/s41598-020-78854-6

Bézière, N., Hardy, M., Poulhès, F., Karoui, H., Tordo, P., Ouari, O., Frapart, Y. M., Rockenbauer, A., Boucher, J. L., Mansuy, D., & Peyrot, F. (2014). Metabolic stability of superoxide adducts derived from newly developed cyclic nitrone spin traps. *Free Radical Biology and Medicine*, *67*, 150–158. https://doi.org/10.1016/J.FREERADBIOMED.2013.10.812

Blanch-Ruiz, M. A., Ortega-Luna, R., Gómez-García, G., Martínez-Cuesta, M. Á., & Álvarez, Á. (2022). Role of neutrophil extracellular traps in COVID-19 progression: An insight for effective treatment. *Biomedicines*, *10*(1). https://doi.org/10.3390/BIOMEDICINES10010031

Bordon, J., Aliberti, S., Fernandez-Botran, R., Uriarte, S. M., Rane, M. J., Duvvuri, P., Peyrani, P., Morlacchi, L. C., Blasi, F., & Ramirez, J. A. (2013). Understanding the roles of cytokines and neutrophil activity and neutrophil apoptosis in the protective versus deleterious inflammatory response in pneumonia. *International Journal of Infectious Diseases*, *17*(2), 76–83. https://doi.org/10.1016/J.IJID.2012.06.006

Bøyum, A., Skrede, K. K., Myhre, O., Tennfjord, V. A., Neurauter, C. G., Tolleshaug, H., Knudsen, E., Opstad, P. K., Bjørås, M., & Benestad, H. B. (2010). Calprotectin (S100A8/S100A9) and myeloperoxidase: Co-regulators of formation of reactive oxygen species. *Toxins*, *2*(1), 95–115. https://doi.org/10.3390/TOXINS2010095

Brinkmann, V., & Zychlinsky, A. (2012). Neutrophil extracellular traps: Is immunity the second function of chromatin? *Journal of Cell Biology*, *198*(5), 773–783. https://doi.org/10.1083/JCB.201203170

Byrd, A. S., O'Brien, X. M., Johnson, C. M., Lavigne, L. M., & Reichner, J. S. (2013). An extracellular matrix–based mechanism of rapid neutrophil extracellular trap formation in response to *Candida albicans*. *The Journal of Immunology*, *190*(8), 4136–4148. https://doi.org/10.4049/JIMMUNOL.1202671

Carestia, A., Frechtel, G., Cerrone, G., Linari, M. A., Gonzalez, C. D., Casais, P., & Schattner, M. (2016). NETosis before and after hyperglycemic control in type 2 diabetes mellitus patients. *PLOS ONE*, *11*(12). https://doi.org/10.1371/JOURNAL.PONE.0168647

Castanheira, F. V. S., & Kubes, P. (2019). Neutrophils and NETs in modulating acute and chronic inflammation. *Blood*, *133*(20), 2178–2185. https://doi.org/10.1182/BLOOD-2018-11-844530

Charkhizadeh, S., Imani, M., Gheibi, N., Shabaani, F., Nikpajouh, A., & Rezvany, M. R. (2020). *In vitro* inhibitory effect of recombinant human calprotectin on Nalm6 leukemia cell line.

Anti-Cancer Agents in Medicinal Chemistry, *20*(8), 951–962. https://doi.org/10.2174/1871520620666200331101209

Chen, Y., Zhang, H., Hu, X., Cai, W., Ni, W., & Zhou, K. (2022). Role of NETosis in central nervous system injury. *Oxidative Medicine and Cellular Longevity*, *2022*. https://doi.org/10.1155/2022/3235524

Chen, Z., Akenhead, M. A., Sun, X., Sapper, H., Shin, H. Y., Hinds, B. J., Chen, Z., Sun, X., Sapper, H., Akenhead, M. A., Shin, H. Y., & Hinds, B. J. (2016). Flow-through electroporation of HL-60 white blood cell suspensions using nanoporous membrane electrodes. *Advanced Healthcare Materials*, *5*(16), 2105–2112. https://doi.org/10.1002/ADHM.201600204

Chu, D., Dong, X., Shi, X., Zhang, C., & Wang, Z. (2018). Neutrophil-based drug delivery systems. *Advanced Materials*, *30*(22). https://doi.org/10.1002/ADMA.201706245

Chu, D., Gao, J., & Wang, Z. (2015). Neutrophil-mediated delivery of therapeutic nanoparticles across blood vessel barrier for treatment of inflammation and infection. *ACS Nano*, *9*(12), 11800–11811. https://doi.org/10.1021/ACSNANO.5B05583/ASSET/IMAGES/LARGE/NN-2015-055834_0009.JPEG

Collins, S. J. (1987). The HL-60 promyelocytic leukemia cell line: Proliferation, differentiation, and cellular oncogene expression. *Blood*, *70*(5), 1233–1244. https://doi.org/10.1182/BLOOD.V70.5.1233.1233

Cools-Lartigue, J., Spicer, J., Najmeh, S., & Ferri, L. (2014). Neutrophil extracellular traps in cancer progression. *Cellular and Molecular Life Sciences*, *71*(21), 4179–4194. https://doi.org/10.1007/S00018-014-1683-3/FIGURES/3

Cruz, M. A., Bohinc, D., Andraska, E. A., Alvikas, J., Raghunathan, S., Masters, N. A., van Kleef, N. D., Bane, K. L., Hart, K., Medrow, K., Sun, M., Liu, H., Haldeman, S., Banerjee, A., Lessieur, E. M., Hageman, K., Gandhi, A., de la Fuente, M., Nieman, M. T., & Stavrou, E. X. (2022). Nanomedicine platform for targeting activated neutrophils and neutrophil-platelet complexes using an α1-antitrypsin-derived peptide motif. *Nature Nanotechnology 2022, 17*(9), 1004–1014. https://doi.org/10.1038/s41565-022-01161-w

Čapek, J., & Roušar, T. (2021). Detection of oxidative stress induced by nanomaterials in cells: The roles of reactive oxygen species and glutathione. *Molecules*, *26*(16), 4710. https://doi.org/10.3390/MOLECULES26164710

Damascena, H. L., Silveira, W. A. A., Castro, M. S., & Fontes, W. (2022). Neutrophil activated by the famous and potent PMA (phorbol myristate acetate). *Cells*, *11*(18), 2889. https://doi.org/10.3390/CELLS11182889/S1

Davies, M. J. (2016). Detection and characterisation of radicals using electron paramagnetic resonance (EPR) spin trapping and related methods. *Methods*, *109*, 21–30. https://doi.org/10.1016/J.YMETH.2016.05.013

DeLeo, F. R., & Allen, L.-A. H. (2020). Phagocytosis and neutrophil extracellular traps. *Faculty Reviews*, *9*. https://doi.org/10.12703/R/9-25

Delgado-Rizo, V., Martínez-Guzmán, M. A., Iñiguez-Gutierrez, L., García-Orozco, A., Alvarado-Navarro, A., & Fafutis-Morris, M. (2017). Neutrophil extracellular traps and its implications in inflammation: An overview. *Frontiers in Immunology*, *8*, 81. https://doi.org/10.3389/FIMMU.2017.00081/BIBTEX

Dewitt, S., & Hallett, M. B. (2020). Calpain activation by Ca^{2+} and its role in phagocytosis. *Advances in Experimental Medicine and Biology*, *1246*, 129–151. https://doi.org/10.1007/978-3-030-40406-2_8/COVER

Ding, J., Zhang, Z., Huang, W., & Bi, G. (2021). Nicotinamide phosphoribosyltransferase inhibitor is a novel therapeutic candidate in LPS-induced neutrophil extracellular traps. *Microbiology and Immunology*, *65*(7), 257–264. https://doi.org/10.1111/1348-0421.12885

Ding, T., Wang, S., Zhang, X., Zai, W., Fan, J., Chen, W., Bian, Q., Luan, J., Shen, Y., Zhang, Y., Ju, D., & Mei, X. (2018). Kidney protection effects of dihydroquercetin on diabetic nephropathy through suppressing ROS and NLRP3 inflammasome. *Phytomedicine*, *41*, 45–53. https://doi.org/10.1016/J.PHYMED.2018.01.026

Douda, D. N., Khan, M. A., Grasemann, H., & Palaniyar, N. (2015). SK3 channel and mitochondrial ROS mediate NADPH oxidase-independent NETosis induced by calcium influx. *Proceedings of the National Academy of Sciences of the United States of America*, *112*(9),

2817–2822. https://doi.org/10.1073/PNAS.1414055112/SUPPL_FILE/PNAS.201414055SI.PDF
Dumanović, J., Nepovimova, E., Natić, M., Kuča, K., & Jaćević, V. (2021). The significance of reactive oxygen species and antioxidant defense system in plants: A concise overview. *Frontiers in Plant Science*, *11*, 2106. https://doi.org/10.3389/FPLS.2020.552969/BIBTEX
Duque, G. A., & Descoteaux, A. (2014). Macrophage cytokines: Involvement in immunity and infectious diseases. *Frontiers in Immunology*, *5*, 491. https://doi.org/10.3389/FIMMU.2014.00491/BIBTEX
El-Benna, J., Hurtado-Nedelec, M., Marzaioli, V., Marie, J.-C., Gougerot-Pocidalo, M.-A., & My-Chan Dang, P. (2016). Priming of the neutrophil respiratory burst: Role in host defense and inflammation. *Immunological Reviews*, *273*(1), 180–193. https://doi.org/10.1111/IMR.12447
Fousert, E., Toes, R., & Desai, J. (2020). Neutrophil Extracellular traps (NETs) take the central stage in driving autoimmune responses. *Cells,* *9*(4), 915. https://doi.org/10.3390/CELLS9040915
Fu, C. H., Tsai, W. C., Lee, T. J., Huang, C. C., Chang, P. H., & Su Pang, J. H. (2016). Simvastatin inhibits IL-5-Induced chemotaxis and CCR3 expression of HL-60-derived and human primary eosinophils. *PLOS ONE*, *11*(6). https://doi.org/10.1371/JOURNAL.PONE.0157186
Galadari, S., Rahman, A., Pallichankandy, S., & Thayyullathil, F. (2017). Reactive oxygen species and cancer paradox: To promote or to suppress? *Free Radical Biology and Medicine*, *104*, 144–164. https://doi.org/10.1016/J.FREERADBIOMED.2017.01.004
Garcia-Senosiain, A., Kana, I. H., Singh, S., Das, M. K., Dziegiel, M. H., Hertegonne, S., Adu, B., & Theisen, M. (2021). Neutrophils dominate in opsonic phagocytosis of *P. falciparum* blood-stage merozoites and protect against febrile malaria. *Communications Biology*, *4*(1), 1–10. https://doi.org/10.1038/s42003-021-02511-5
Garley, M., Jabłońska, E., & Dąbrowska, D. (2016). NETs in cancer. *Tumor Biology*, *37*(11), 14355–14361. https://doi.org/10.1007/S13277-016-5328-Z/FIGURES/1
Gazendam, R. P., van de Geer, A., Roos, D., van den Berg, T. K., & Kuijpers, T. W. (2016). How neutrophils kill fungi. *Immunological Reviews*, *273*(1), 299–311. https://doi.org/10.1111/IMR.12454
Giaglis, S., Hahn, S., & Hasler, P. (2016). The NET outcome: Are neutrophil extracellular traps of any relevance to the pathophysiology of autoimmune disorders in childhood? *Frontiers in Pediatrics*, *4*. https://doi.org/10.3389/FPED.2016.00097
Gilda, J. E., Ghosh, R., Cheah, J. X., West, T. M., Bodine, S. C., & Gomes, A. V. (2015). Western blotting inaccuracies with unverified antibodies: Need for a western blotting minimal reporting standard (WBMRS). *PLOS ONE*, *10*(8). https://doi.org/10.1371/JOURNAL.PONE.0135392
Gray, R. D., Lucas, C. D., Mackellar, A., Li, F., Hiersemenzel, K., Haslett, C., Davidson, D. J., & Rossi, A. G. (2013). Activation of conventional protein kinase C (PKC) is critical in the generation of human neutrophil extracellular traps. *Journal of Inflammation*, *10*(1), 1–8. https://doi.org/10.1186/1476-9255-10-12/FIGURES/5
Gupta, A. K., Giaglis, S., Hasler, P., & Hahn, S. (2014). Efficient neutrophil extracellular trap induction requires mobilization of both intracellular and extracellular calcium pools and is modulated by cyclosporine A. *PLOS ONE*, *9*(5). https://doi.org/10.1371/JOURNAL.PONE.0097088
Hakkim, A., Fürnrohr, B. G., Amann, K., Laube, B., Abed, U. A., Brinkmann, V., Herrmann, M., Voll, R. E., & Zychlinsky, A. (2010). Impairment of neutrophil extracellular trap degradation is associated with lupus nephritis. *Proceedings of the National Academy of Sciences of the United States of America*, *107*(21), 9813–9818. https://doi.org/10.1073/PNAS.0909927107/-/DCSUPPLEMENTAL
Halverson, T. W. R., Wilton, M., Poon, K. K. H., Petri, B., & Lewenza, S. (2015). DNA is an antimicrobial component of neutrophil extracellular traps. *PLOS Pathogens*, *11*(1). https://doi.org/10.1371/JOURNAL.PPAT.1004593
Hamam, H. J., Khan, M. A., & Palaniyar, N. (2019). Histone acetylation promotes neutrophil extracellular trap formation. *Biomolecules, 9*(1), 32. https://doi.org/10.3390/BIOM9010032

Hasan, R., Rink, L., & Haase, H. (2016). Chelation of free Zn^{2+} impairs chemotaxis, phagocytosis, oxidative burst, degranulation, and cytokine production by neutrophil granulocytes. *Biological Trace Element Research*, *171*(1), 79–88. https://doi.org/10.1007/S12011-015-0515-0/FIGURES/5

He, F. (2011). BCA (Bicinchoninic Acid) protein assay. *BIO-PROTOCOL*, *1*(5). https://doi.org/10.21769/BIOPROTOC.44

Heinrich, V., & Lee, C. Y. (2011). Blurred line between chemotactic chase and phagocytic consumption: An immunophysical single-cell perspective. *Journal of Cell Science*, *124*(18), 3041–3051. https://doi.org/10.1242/JCS.086413

Hernandes, M. S., D'Avila, J. C., Trevelin, S. C., Reis, P. A., Kinjo, E. R., Lopes, L. R., Castro-Faria-Neto, H. C., Cunha, F. Q., Britto, L. R. G., & Bozza, F. A. (2014). The role of NOX2-derived ROS in the development of cognitive impairment after sepsis. *Journal of Neuroinflammation*, *11*(1), 1–12. https://doi.org/10.1186/1742-2094-11-36/FIGURES/8

Hidalgo, A., Chilvers, E. R., Summers, C., & Koenderman, L. (2019). The neutrophil life cycle. *Trends in Immunology*, *40*(7), 584–597. https://doi.org/10.1016/J.IT.2019.04.013

Hoesel, B., & Schmid, J. A. (2013). The complexity of NF-κB signaling in inflammation and cancer. *Molecular Cancer, 12*(1), 1–15. https://doi.org/10.1186/1476-4598-12-86

Hou, W., Wang, Z. Y., Lin, J., & Chen, W. M. (2020). Induction of differentiation of the acute myeloid leukemia cell line (HL-60) by a securinine dimer. *Cell Death Discovery, 6*(1), 1–11. https://doi.org/10.1038/s41420-020-00354-3

Huang, Q., Wang, L., Ran, Q., Wang, J., Wang, C., He, H., Li, L., & Qi, H. (2019). Notopterol-induced apoptosis and differentiation in human acute myeloid leukemia HL-60 cells. *Drug Design, Development and Therapy*, *13*, 1927–1940. https://doi.org/10.2147/DDDT.S189969

Hyun, Y.-M., & Hong, C.-W. (2017). Deep insight into neutrophil trafficking in various organs. *Journal of Leukocyte Biology*, *102*(3), 617–629. https://doi.org/10.1189/JLB.1RU1216-521R

Ipek, E., Yolcu, M., Yildirim, E., Altinkaynak, K., Sebin, S. O., Kalkan, K., Gulcu, O., Ermis, E., & Ozturk, M. (2018). A novel marker of inflammation: Azurocidin in patients with ST segment elevation myocardial infarction. *International Journal of Molecular Sciences*, *19*(12). https://doi.org/10.3390/IJMS19123797

Ireland, A. S., & Oliver, T. G. (2020). Neutrophils create an impeNETrable shield between tumor and cytotoxic immune cells. *Immunity*, *52*(5), 729–731. https://doi.org/10.1016/J.IMMUNI.2020.04.009

Jaumouillé, V., & Waterman, C. M. (2020). Physical constraints and forces involved in phagocytosis. *Frontiers in Immunology*, *11*, 1097. https://doi.org/10.3389/FIMMU.2020.01097/BIBTEX

Juan, C. A., de la Lastra, J. M. P., Plou, F. J., & Pérez-Lebeña, E. (2021). The chemistry of reactive oxygen species (ROS) revisited: Outlining their role in biological macromolecules (DNA, Lipids and Proteins) and induced pathologies. *International Journal of Molecular Sciences*, *22*(9). https://doi.org/10.3390/IJMS22094642

Kasus-Jacobi, A., Land, C. A., Stock, A. J., Washburn, J. L., & Anne Pereira, H. (2020). Antimicrobial peptides derived from the immune defense protein CAP37 inhibit TLR-4 activation by S100A9. *Investigative Ophthalmology & Visual Science*, *61*(4), 16–16. https://doi.org/10.1167/IOVS.61.4.16

Keshari, R. S., Verma, A., Barthwal, M. K., & Dikshit, M. (2013). Reactive oxygen species-induced activation of ERK and p38 MAPK mediates PMA-induced NETs release from human neutrophils. *Journal of Cellular Biochemistry*, *114*(3), 532–540. https://doi.org/10.1002/JCB.24391

Klebanoff, S. J., Kettle, A. J., Rosen, H., Winterbourn, C. C., & Nauseef, W. M. (2013). Myeloperoxidase: A front-line defender against phagocytosed microorganisms. *Journal of Leukocyte Biology*, *93*(2), 185–198. https://doi.org/10.1189/JLB.0712349

Koyama, S., Narita, E., Suzuki, Y., Taki, M., Shinohara, N., & Miyakoshi, J. (2015). Effect of a 2.45-GHz radiofrequency electromagnetic field on neutrophil chemotaxis and phagocytosis in differentiated human HL-60 cells. *Journal of Radiation Research*, *56*(1), 30–36. https://doi.org/10.1093/JRR/RRU075

Koyani, C. N., Flemmig, J., Malle, E., & Arnhold, J. (2015). Myeloperoxidase scavenges peroxynitrite: A novel anti-inflammatory action of the heme enzyme. *Archives of Biochemistry and Biophysics*, *571*, 1–9. https://doi.org/10.1016/J.ABB.2015.02.028

Kuwabara, W. M. T., Zhang, L., Schuiki, I., Curi, R., Volchuk, A., & Alba-Loureiro, T. C. (2015). NADPH oxidase-dependent production of reactive oxygen species induces endoplasmatic reticulum stress in neutrophil-like HL-60 cells. *PLOS ONE*, *10*(2). https://doi.org/10.1371/JOURNAL.PONE.0116410

Lahoz-Beneytez, J., Elemans, M., Zhang, Y., Ahmed, R., Salam, A., Block, M., Niederalt, C., Asquith, B., & Macallan, D. (2016). Human neutrophil kinetics: Modeling of stable isotope labeling data supports short blood neutrophil half-lives. *Blood*, *127*(26), 3431–3438. https://doi.org/10.1182/BLOOD-2016-03-700336

Lázaro-Díez, M., Chapartegui-González, I., Suberbiola, B., Ocejo-Vinyals, J. G., López-Hoyos, M., & Ramos-Vivas, J. (2020). Gene expression profiling in human neutrophils after infection with *Acinetobacter baumannii in vitro*. *PLOS ONE*, *15*(11). https://doi.org/10.1371/JOURNAL.PONE.0242674

Lee, W. Bin, Yan, J. J., Kang, J. S., Chung, S., & Kim, L. K. (2017). Mycobacterial cord factor enhances migration of neutrophil-like HL-60 cells by prolonging AKT phosphorylation. *Microbiology and Immunology*, *61*(12), 523–530. https://doi.org/10.1111/1348-0421.12544

Liao, C. C., Chang, Y. S., Cheng, C. W., Chi, W. M., Tsai, K. L., Chen, W. J., Kung, T. S., Tai, C. C., Lin, Y. F., Lin, H. T., Lu, Y. Y., & Lin, C. Y. (2018). Isotypes of autoantibodies against differentially expressed novel malondialdehyde-modified peptide adducts in serum of Taiwanese women with rheumatoid arthritis. *Journal of Proteomics*, *170*, 141–150. https://doi.org/10.1016/J.JPROT.2017.08.012

Lood, C., Blanco, L. P., Purmalek, M. M., Carmona-Rivera, C., De Ravin, S. S., Smith, C. K., Malech, H. L., Ledbetter, J. A., Elkon, K. B., & Kaplan, M. J. (2016). Neutrophil extracellular traps enriched in oxidized mitochondrial DNA are interferogenic and contribute to lupus-like disease. *Nature Medicine, 22*(2), 146–153. https://doi.org/10.1038/nm.4027

Ma, Y., Yabluchanskiy, A., & Lindsey, M. L. (2013). Neutrophil roles in left ventricular remodeling following myocardial infarction. *Fibrogenesis and Tissue Repair*, *6*(1), 1–10. https://doi.org/10.1186/1755-1536-6-11/FIGURES/3

Ma, Y., Zhang, Y., & Zhu, L. (2021). Role of neutrophils in acute viral infection. *Immunity, Inflammation and Disease*, *9*(4), 1186. https://doi.org/10.1002/IID3.500

Majewski, P., Majchrzak-Gorecka, M., Grygier, B., Skrzeczynska-Moncznik, J., Osiecka, O., & Cichy, J. (2016). Inhibitors of serine proteases in regulating the production and function of neutrophil extracellular traps. *Frontiers in Immunology*, *7*, 261. https://doi.org/10.3389/FIMMU.2016.00261/BIBTEX

Malech, H. L., Deleo, F. R., & Quinn, M. T. (2014). The role of neutrophils in the immune system: An overview. *Methods in Molecular Biology*, *1124*, 3–10. https://doi.org/10.1007/978-1-62703-845-4_1/COVER

Manda-Handzlik, A., Bystrzycka, W., Wachowska, M., Sieczkowska, S., Stelmaszczyk-Emmel, A., Demkow, U., & Ciepiela, O. (2018). The influence of agents differentiating HL-60 cells toward granulocyte-like cells on their ability to release neutrophil extracellular traps. *Immunology and Cell Biology*, *96*(4), 413–425. https://doi.org/10.1111/IMCB.12015

Mandic, M., Misirkic Marjanovic, M., Vucicevic, L., Jovanovic, M., Bosnjak, M., Perovic, V., Ristic, B., Ciric, D., Harhaji-Trajkovic, L., & Trajkovic, V. (2022). MAP kinase-dependent autophagy controls phorbol myristate acetate-induced macrophage differentiation of HL-60 leukemia cells. *Life Sciences*, *297*. https://doi.org/10.1016/J.LFS.2022.120481

Manoharan, R. R., Sedlářová, M., Pospíšil, P., & Prasad, A. (2023). Detection and characterization of free oxygen radicals induced protein adduct formation in differentiating macrophages. *Biochimica et Biophysica Acta (BBA) – General Subjects*, *1867*(5). https://doi.org/10.1016/J.BBAGEN.2023.130324

Mas-Bargues, C., Escrivá, C., Dromant, M., Borrás, C., & Viña, J. (2021). Lipid peroxidation as measured by chromatographic determination of malondialdehyde. Human plasma reference values in health and disease. *Archives of Biochemistry and Biophysics*, *709*, 108941. https://doi.org/10.1016/J.ABB.2021.108941

Maspi, N., Abdoli, A., & Ghaffarifar, F. (2016). Pro- and anti-inflammatory cytokines in cutaneous leishmaniasis: A review. *Pathogens and Global Health*, *110*(6), 247–260. https://doi.org/10.1080/20477724.2016.1232042

McDonnell, A. M., & Dang, C. H. (2013). Basic review of the cytochrome P450 system. *Journal of the Advanced Practitioner in Oncology*, *4*(4), 263. https://doi.org/10.6004/JADPRO.2013.4.4.7

McTague, A., Tazhitdinova, R., & Timoshenko, A. V. (2022). O-GlcNAc-mediated regulation of galectin expression and secretion in human promyelocytic HL-60 cells undergoing neutrophilic differentiation. *Biomolecules 2022, 12*(12), 1763. https://doi.org/10.3390/BIOM12121763

Mirończuk-Chodakowska, I., Witkowska, A. M., & Zujko, M. E. (2018). Endogenous non-enzymatic antioxidants in the human body. *Advances in Medical Sciences*, *63*(1), 68–78. https://doi.org/10.1016/J.ADVMS.2017.05.005

Moris, D., Spartalis, M., Spartalis, E., Karachaliou, G. S., Karaolanis, G. I., Tsourouflis, G., Tsilimigras, D. I., Tzatzaki, E., & Theocharis, S. (2017). The role of reactive oxygen species in the pathophysiology of cardiovascular diseases and the clinical significance of myocardial redox. *Annals of Translational Medicine*, *5*(16). https://doi.org/10.21037/ATM.2017.06.27

Mroczek, A., Cieloch, A., Manda-Handzlik, A., Kuźmicka, W., Muchowicz, A., & Wachowska, M. (2020). Overexpression of ATG5 gene makes granulocyte-like HL-60 susceptible to release reactive oxygen species. *International Journal of Molecular Sciences, 21*(15), 5194. https://doi.org/10.3390/IJMS21155194

Nadeem, A., Ahmad, S. F., Bakheet, S. A., Al-Harbi, N. O., AL-Ayadhi, L. Y., Attia, S. M., & Zoheir, K. M. A. (2017). Toll-like receptor 4 signaling is associated with upregulated NADPH oxidase expression in peripheral T-cells of children with autism. *Brain, Behavior, and Immunity*, *61*, 146–154. https://doi.org/10.1016/J.BBI.2016.12.024

Nalmpantis, D., Gatou, A., Fragkioudakis, I., Margariti, A., Skoura, L., & Sakellari, D. (2020). Azurocidin in gingival crevicular fluid as a potential biomarker of chronic periodontitis. *Journal of Periodontal Research*, *55*(2), 209–214. https://doi.org/10.1111/JRE.12703

Nascimento, C. R., Rodrigues Fernandes, N. A., Gonzalez Maldonado, L. A., & Rossa Junior, C. (2022). Comparison of monocytic cell lines U937 and THP-1 as macrophage models for *in vitro* studies. *Biochemistry and Biophysics Reports*, *32*. https://doi.org/10.1016/J.BBREP.2022.101383

Nawab, A., Nichols, A., Klug, R., Shapiro, J. I., & Sodhi, K. (2017). Spin trapping: A review for the study of obesity related oxidative stress and Na^+/K^+-ATPase. *Journal of Clinical & Cellular Immunology*, *8*(3). https://doi.org/10.4172/2155-9899.1000505

Niemiec, M. J., de Samber, B., Garrevoet, J., Vergucht, E., Vekemans, B., de Rycke, R., Björn, E., Sandblad, L., Wellenreuther, G., Falkenberg, G., Cloetens, P., Vincze, L., & Urban, C. F. (2015). Trace element landscape of resting and activated human neutrophils on the sub-micrometer level. *Metallomics*, *7*(6), 996–1010. https://doi.org/10.1039/C4MT00346B

Nizer, W. S. da C., Inkovskiy, V., & Overhage, J. (2020). Surviving reactive chlorine stress: Responses of gram-negative bacteria to hypochlorous acid. *Microorganisms*, *8*(8), 1–27. https://doi.org/10.3390/MICROORGANISMS8081220

van der Paal, J., Neyts, E. C., Verlackt, C. C. W., & Bogaerts, A. (2015). Effect of lipid peroxidation on membrane permeability of cancer and normal cells subjected to oxidative stress. *Chemical Science*, *7*(1), 489–498. https://doi.org/10.1039/C5SC02311D

Papac-Milicevic, N., Busch, C. J. L., & Binder, C. J. (2016). Malondialdehyde epitopes as targets of immunity and the implications for atherosclerosis. *Advances in Immunology*, *131*, 1–59. https://doi.org/10.1016/BS.AI.2016.02.001

Perera, C., McNeil, H. P., & Geczy, C. L. (2010). S100 calgranulins in inflammatory arthritis. *Immunology and Cell Biology*, *88*(1), 41–49. https://doi.org/10.1038/ICB.2009.88

Pieterse, E., Rother, N., Yanginlar, C., Hilbrands, L. B., & van der Vlag, J. (2016). Neutrophils discriminate between lipopolysaccharides of different bacterial sources and selectively release neutrophil extracellular traps. *Frontiers in Immunology*, *7*, 484. https://doi.org/10.3389/FIMMU.2016.00484/BIBTEX

Poplutz, M. K., Wessels, I., Rink, L., & Uciechowski, P. (2014). Regulation of the Interleukin-6 gene expression during monocytic differentiation of HL-60 cells by chromatin remodeling and methylation. *Immunobiology*, *219*(8), 619–626. https://doi.org/10.1016/J.IMBIO.2014.03.016

Porto, B. N., & Stein, R. T. (2016). Neutrophil extracellular traps in pulmonary diseases: Too much of a good thing? *Frontiers in Immunology*, *7*, 311. https://doi.org/10.3389/FIMMU.2016.00311/BIBTEX

Pospíšil, P. (2016). Production of reactive oxygen species by photosystem II as a response to light and temperature stress. *Frontiers in Plant Science*, *7*, 1950. https://doi.org/10.3389/FPLS.2016.01950/BIBTEX

Prasad, A., Manoharan, R. R., Sedlářová, M., & Pospíšil, P. (2021). Free radical-mediated protein radical formation in differentiating monocytes. *International Journal of Molecular Sciences*, *22*(18), 9963. https://doi.org/10.3390/IJMS22189963/S1

Prat, C., Bouvier, D., Comptour, A., Marceau, G., Belville, C., Clairefond, G., Blanc, P., Gallot, D., Blanchon, L., & Sapin, V. (2015). All-trans-retinoic acid regulates aquaporin-3 expression and related cellular membrane permeability in the human amniotic environment. *Placenta*, *36*(8), 881–887. https://doi.org/10.1016/J.PLACENTA.2015.05.010

Ramachandran, R. P., Madhivanan, S., Sundararajan, R., Wan-Ying Lin, C., & Sankaranarayanan, K. (2014). An *in vitro* study of electroporation of leukemia and cervical cancer cells. *Electroporation-Based Therapies for Cancer*, 161–183. https://doi.org/10.1533/9781908818294.161

Ramadass, M., & Catz, S. D. (2016). Molecular mechanisms regulating secretory organelles and endosomes in neutrophils and their implications for inflammation. *Immunological Reviews*, *273*(1), 249–265. https://doi.org/10.1111/IMR.12452

Rawat, K., Syeda, S., & Shrivastava, A. (2021). Neutrophil-derived granule cargoes: Paving the way for tumor growth and progression. *Cancer and Metastasis Reviews, 40*(1), 221–244. https://doi.org/10.1007/S10555-020-09951-1

Razvina, O., Jiang, S., Matsubara, K., Ohashi, R., Hasegawa, G., Aoyama, T., Daigo, K., Kodama, T., Hamakubo, T., & Naito, M. (2015). Differential expression of pentraxin 3 in neutrophils. *Experimental and Molecular Pathology*, *98*(1), 33–40. https://doi.org/10.1016/J.YEXMP.2014.11.009

Redza-Dutordoir, M., & Averill-Bates, D. A. (2016). Activation of apoptosis signalling pathways by reactive oxygen species. *Biochimica et Biophysica Acta (BBA) – Molecular Cell Research*, *1863*(12), 2977–2992. https://doi.org/10.1016/J.BBAMCR.2016.09.012

Rincón, E., Rocha-Gregg, B. L., & Collins, S. R. (2018). A map of gene expression in neutrophil-like cell lines. *BMC Genomics*, *19*(1), 1–17. https://doi.org/10.1186/S12864-018-4957-6/FIGURES/6

Roessler, M. M., & Salvadori, E. (2018). Principles and applications of EPR spectroscopy in the chemical sciences. *Chemical Society Reviews*, *47*(8), 2534–2553. https://doi.org/10.1039/C6CS00565r

Rosales, C. (2018). Neutrophil: A cell with many roles in inflammation or several cell types? *Frontiers in Physiology*, *9*, 113. https://doi.org/10.3389/FPHYS.2018.00113/BIBTEX

Rosales, C., Demaurex, N., Lowell, C. A., & Uribe-Querol, E. (2016). Neutrophils: Their role in innate and adaptive immunity. *Journal of Immunology Research*, *2016*. https://doi.org/10.1155/2016/1469780

Ruiz-Alcaraz, A. J., Martínez-Sánchez, M. A., García-Peñarrubia, P., Martinez-Esparza, M., Ramos-Molina, B., & Moreno, D. A. (2022). Analysis of the anti-inflammatory potential of *Brassica* bioactive compounds in a human macrophage-like cell model derived from HL-60 cells. *Biomedicine & Pharmacotherapy*, *149*. https://doi.org/10.1016/J.BIOPHA.2022.112804

Salvioli, S., Storci, G., Pinti, M., Quaglino, D., Moretti, L., Merlo-Pich, M., Lenaz, G., Filosa, S., Fico, A., Bonafè, M., Monti, D., Troiano, L., Nasi, M., Cossarizza, A., & Franceschi, C. (2003). Apoptosis-resistant phenotype in HL-60-derived cells HCW-2 is related to changes in expression of stress-induced proteins that impact on redox status and mitochondrial metabolism. *Cell Death & Differentiation, 10*(2), 163–174. https://doi.org/10.1038/sj.cdd.4401124

Savchenko, A. S., Martinod, K., Seidman, M. A., Wong, S. L., Borissoff, J. I., Piazza, G., Libby, P., Goldhaber, S. Z., Mitchell, R. N., & Wagner, D. D. (2014). Neutrophil extracellular traps form predominantly during the organizing stage of human venous thromboembolism development. *Journal of Thrombosis and Haemostasis*, *12*(6), 860–870. https://doi.org/10.1111/JTH.12571

Schieber, M., & Chandel, N. S. (2014). ROS function in redox signaling and oxidative stress. *Current Biology*, *24*(10), 453–462. https://doi.org/10.1016/J.CUB.2014.03.034

Schumann, J. (2016). It is all about fluidity: Fatty acids and macrophage phagocytosis. *European Journal of Pharmacology*, *785*, 18–23. https://doi.org/10.1016/J.EJPHAR.2015.04.057

Shaikh, R., Pund, M., Dawane, A., & Iliyas, S. (2014). Evaluation of anticancer, antioxidant, and possible anti-inflammatory properties of selected medicinal plants used in Indian traditional medication. *Journal of Traditional and Complementary Medicine*, *4*(4), 253–257. https://doi.org/10.4103/2225-4110.128904

Shirai, A., Sugiyama, Y., & Rieu, J. P. (2018). Differentiation of neutrophil-like HL-60 cells strongly impacts their rolling on surfaces with various adhesive properties under a pressing force. *Technology and Health Care*, *26*(1), 93–108. https://doi.org/10.3233/THC-171052

Soehnlein, O., Steffens, S., Hidalgo, A., & Weber, C. (2017). Neutrophils as protagonists and targets in chronic inflammation. *Nature Reviews Immunology, 17*(4), 248–261. https://doi.org/10.1038/nri.2017.10

Sprenkeler, E. G. G., Zandstra, J., van Kleef, N. D., Goetschalckx, I., Verstegen, B., Aarts, C. E. M., Janssen, H., Tool, A. T. J., van Mierlo, G., van Bruggen, R., Jongerius, I., & Kuijpers, T. W. (2022). S100A8/A9 is a marker for the release of neutrophil extracellular traps and induces neutrophil activation. *Cells, 11*(2), 236. https://doi.org/10.3390/CELLS11020236

Stefanatos, R., & Sanz, A. (2018). The role of mitochondrial ROS in the aging brain. *FEBS Letters*, *592*(5), 743–758. https://doi.org/10.1002/1873-3468.12902

Stoiber, W., Obermayer, A., Steinbacher, P., & Krautgartner, W. D. (2015). The role of reactive oxygen species (ROS) in the formation of extracellular traps (ETs) in humans. *Biomolecules*, *5*(2), 702. https://doi.org/10.3390/BIOM5020702

Storisteanu, D. M. L., Pocock, J. M., Cowburn, A. S., Juss, J. K., Nadesalingam, A., Nizet, V., & Chilvers, E. R. (2017). Evasion of neutrophil extracellular traps by respiratory pathogens. *American Journal of Respiratory Cell and Molecular Biology*, *56*(4), 423–431. https://doi.org/10.1165/RCMB.2016-0193PS/SUPPL_FILE/DISCLOSURES.PDF

Tasseff, R., Jensen, H. A., Congleton, J., Dai, D., Rogers, K. V., Sagar, A., Bunaciu, R. P., Yen, A., & Varner, J. D. (2017). An effective model of the retinoic acid induced HL-60 differentiation program. *Scientific Reports 7*(1), 1–21. https://doi.org/10.1038/s41598-017-14523-5

Tecchio, C., Micheletti, A., & Cassatella, M. A. (2014). Neutrophil-derived cytokines: Facts beyond expression. *Frontiers in Immunology*, *5*, 508. https://doi.org/10.3389/FIMMU.2014.00508/BIBTEX

Thiam, H. R., Wong, S. L., Wagner, D. D., & Waterman, C. M. (2020). Cellular mechanisms of NETosis. *Annual Review of Cell and Developmental Biology*, *36*, 191–218. https://doi.org/10.1146/ANNUREV-CELLBIO-020520-111016

Tsourouktsoglou, T. D., Warnatsch, A., Ioannou, M., Hoving, D., Wang, Q., & Papayannopoulos, V. (2020). Histones, DNA, and citrullination promote neutrophil extracellular trap inflammation by regulating the localization and activation of TLR4. *Cell Reports*, *31*(5), 107602. https://doi.org/10.1016/J.CELREP.2020.107602

Turner, M. D., Nedjai, B., Hurst, T., & Pennington, D. J. (2014). Cytokines and chemokines: At the crossroads of cell signalling and inflammatory disease. *Biochimica et Biophysica Acta (BBA) – Molecular Cell Research*, *1843*(11), 2563–2582. https://doi.org/10.1016/J.BBAMCR.2014.05.014

Vorobjeva, N. V., & Pinegin, B. V. (2014). Neutrophil extracellular traps: Mechanisms of formation and role in health and disease. *Biochemistry (Moscow)*, *79*(12), 1286–1296. https://doi.org/10.1134/S0006297914120025/METRICS

Wang, H., Zang, J., Zhao, Z., Zhang, Q., & Chen, S. (2021). The advances of neutrophil-derived effective drug delivery systems: A key review of managing tumors and inflammation. *International Journal of Nanomedicine*, *16*, 7663. https://doi.org/10.2147/IJN.S328705

Wang, X., Qin, W., Xu, X., Xiong, Y., Zhang, Y., Zhang, H., & Sun, B. (2017). Endotoxin-induced autocrine ATP signaling inhibits neutrophil chemotaxis through enhancing myosin light chain phosphorylation. *Proceedings of the National Academy of Sciences of the United States of America*, *114*(17), 4483–4488. https://doi.org/10.1073/PNAS.1616752114/SUPPL_FILE/PNAS.1616752114.SM02.WMV

Wang, Y., Chuang, C. Y., Hawkins, C. L., & Davies, M. J. (2022). Activation and inhibition of human matrix metalloproteinase-9 (MMP9) by HOCl, myeloperoxidase and chloramines. *Antioxidants*, *11*(8), 1616. https://doi.org/10.3390/ANTIOX11081616/S1

Witko-Sarsat, V., Rieu, P., Descamps-Latscha, B., Lesavre, P., & Halbwachs-Mecarelli, L. (2000). Neutrophils: Molecules, functions and pathophysiological aspects. *Laboratory Investigation*, *80*(5), 617–654. https://doi.org/10.1038/LABINVEST.3780067

Yin, C., & Heit, B. (2017). Armed for destruction: Formation, function and trafficking of neutrophil granules. *Cell and Tissue Research,* *371*(3), 455–471. https://doi.org/10.1007/S00441-017-2731-8

Zamani, F., Shahneh, F. Z., Aghebati-Maleki, L., & Baradaran, B. (2013). Induction of CD14 expression and differentiation to monocytes or mature macrophages in promyelocytic cell lines: New approach. *Advanced Pharmaceutical Bulletin*, *3*(2), 329. https://doi.org/10.5681/APB.2013.053

Zarkovic, N., Cipak, A., Jaganjac, M., Borovic, S., & Zarkovic, K. (2013). Pathophysiological relevance of aldehydic protein modifications. *Journal of Proteomics*, *92*, 239–247. https://doi.org/10.1016/J.JPROT.2013.02.004

Zha, C., Meng, X., Li, L., Mi, S., Qian, D., Li, Z., Wu, P., Hu, S., Zhao, S., Cai, J., & Liu, Y. (2020). Neutrophil extracellular traps mediate the crosstalk between glioma progression and the tumor microenvironment via the HMGB1/RAGE/IL-8 axis. *Cancer Biology & Medicine*, *17*(1), 154. https://doi.org/10.20892/J.ISSN.2095-3941.2019.0353

Zhang, N., Aiyasiding, X., Li, W. J., Liao, H. H., & Tang, Q. Z. (2022). Neutrophil degranulation and myocardial infarction. *Cell Communication and Signaling,* *20*(1), 1–23. https://doi.org/10.1186/S12964-022-00824-4

Zhong, S., Li, L., Shen, X., Li, Q., Xu, W., Wang, X., Tao, Y., & Yin, H. (2019). An update on lipid oxidation and inflammation in cardiovascular diseases. *Free Radical Biology and Medicine*, *144*, 266–278. https://doi.org/10.1016/J.FREERADBIOMED.2019.03.036

Zhong, W., Sit, W. H., Wan, J. M. F., & Yu, A. C. H. (2011). Sonoporation-induced apoptosis and cell cycle arrest: Initial findings. *AIP Conference Proceedings*, *1359*, 312–317. https://doi.org/10.1063/1.3607924

Zhong, X., Zhao, X., Zhang, L., Liu, N., Shi, S., & Wang, Y. (2022). Sodium hydrosulfide inhibiting endothelial cells injury and neutrophils activation via IL-8/CXCR2/ROS/NF-κB axis in type 1 diabetes mellitus rat. *Biochemical and Biophysical Research Communications*, *606*, 1–9. https://doi.org/10.1016/J.BBRC.2022.03.072

Zuo, Y., Yalavarthi, S., Shi, H., Gockman, K., Zuo, M., Madison, J. A., Blair, C., Weber, A., Barnes, B. J., Egeblad, M., Woods, R. J., Kanthi, Y., & Knight, J. S. (2020). Neutrophil extracellular traps in COVID-19. *JCI Insight*, *5*(11). https://doi.org/10.1172/JCI.INSIGHT.138999

8 LIST OF ABBREVIATIONS

4-HNE	4-hydroxynonenal
AA	acrylamide
APS	ammonium persulfate
ATRA	all-trans retinoic acid
a. u.	arbitrary unit
BCA	bicinchoninic acid
BSA	bovine serum albumin
CAP37	cationic antimicrobial protein of 37 kDa
CLSM	confocal laser scanning microscopy
CYP	cytochrome P450
DIC	differential interference contrast
DMPO	3,4-dihydro-2,3-dimethyl-2*H*-pyrrole-1-oxide
DMSO	dimethyl sulfoxide
DTT	dithiothreitol
EMPO	2-ethoxycarbonyl-2-methyl-3,4-dihydro-2*H*-pyrrole-1-oxide
EPR	electron paramagnetic resonance
FBS	fetal bovine serum
GM-CSF	granulocyte-macrophage colony-stimulating factor
HIF-1	hypoxia-inducible factor-1
HL (HL-60)	human leukaemia
HPLC	high-performance liquid chromatography
HRP	horseradish peroxidase
IL	interleukin
LPS	lipopolysaccharides
MDA	malondialdehyde
MPO	myeloperoxidase
MTT	3-(4,5-dimethylthiazol-2-yl)-2,5-diphenyltetrazolium bromide
NETs	neutrophil extracellular traps
NETosis	neutrophil extracellular traps formation
NF-κB	nuclear factor kappa B
NOX	NADPH oxidase
NP-40	nonyl phenoxypolyethoxylethanol

PBS	phosphate buffer saline
PKC	protein kinase C
PMA	phorbol-12-myristate-13-acetate
PMNs	polymorphonuclear leukocytes
RA	rheumatoid arthritis
RIPA	radioimmunoprecipitation assay
ROS	reactive oxygen species
RPMI	Roswell Park Memorial Institute
RT	room temperature
RT-PCR	real-time polymerase chain reaction
SE	standard error
SEM	scanning electron microscopy
SOD	superoxide dismutase
STEMI	ST segment elevation myocardial infarction
TEM	transmission electron microscopy
TEMED	*N,N,N′,N′*-tetramethylethane-1,2-diamine
TGS	Tris + glycine + sodium dodecyl sulphate
TNF	tumour necrosis factor
Tris	Tris-(hydroxyethyl)-aminomethane